이 학 석 사 학 위 논 문

Toward Sustainability Assessment of Agricultural Ecosystem based on Thermodynamic Approach: A Case Study for Haenam Farmland in Korea

열역학적 접근에 기반한 농업생태계 지속가능성 평가를 향하여 :
한국 해남 농경지 사례 연구

February 2015

서울대학교 대학원
협동과정 농림기상학
Yohana Maria Indrawati

TOWARD SUSTAINABILITY ASSESSMENT OF AGRICULTURAL ECOSYSTEM BASED ON THERMODYNAMIC APPROACH: A CASE STUDY FOR HAENAM FARMLAND IN KOREA

UNDER THE SUPERVISION OF
PROFESSOR JOON KIM

SUBMITTED TO THE FACULTY OF THE GRADUATE SCHOOL
OF SEOUL NATIONAL UNIVERSITY

BY
YOHANA MARIA INDRAWATI

INTERDISCIPLINARY PROGRAM IN
AGRICULTURAL AND FOREST METEOROLOGY

DECEMBER 2014

APPROVED AS A QUALIFIED THESIS OF
YOHANA MARIA INDRAWATI

FOR THE DEGREE OF MASTER OF SCIENCE
IN AGRICULTURAL AND FOREST METEOROLOGY
BY COMMITTEE MEMBERS

JANUARY 2015

CHAIRMAN _____
Kwang Soo Kim, Ph.D.

VICE-CHAIRMAN _____
Joon Kim, Ph.D.

MEMBER _____
Youngryel Ryu, Ph.D.

ABSTRACT

Toward Sustainability Assessment of Agricultural Ecosystem based on Thermodynamic Approach: A Case Study for Haenam Farmland in Korea

Yohana Maria Indrawati

Interdisciplinary Program in Agricultural and Forest Meteorology

The Graduate School of Seoul National University

An assessment of sustainability in an agricultural ecosystem is necessary to find out whether the current setting of the system under human intervention is a proper configuration toward sustainable management. This research attempted to utilize the long-term monitoring dataset of eddy covariance (*EC*) measurement in a typical agricultural ecosystem to quantify the ecosystem performance particularly in water use. The specific objectives were (1) to document decadal climatology, water use, energy, and carbon balance, and (2) to assess the state of this agricultural ecosystem based on thermodynamic perspective. The question is how to describe the current state of water use in an agricultural ecosystem and the dynamic under human management. This research was conducted by using eddy covariance measurement data for a decade in an agricultural ecosystem in Korea (Haenam Farmland in Korea, HFK).

The mean annual precipitation (P) was 1454 ± 188 mm of which more than 53% occurred during the summer season. The mean annual downward shortwave radiation ($R_{s\downarrow}$) was 5025 ± 154 MJ m^{-2} whereas that of air temperature (T_a) was 13.6 ± 0.1 ˚C with a gradually increasing pattern. Footprint climatology showed that most of the measured fluxes were from less than 200 meter around the tower. The Budyko curve indicated that the actual evapotranspiration (ET) is limited by the available energy. The annual ET was 639 ± 32 mm while the annual reference ET (ET_o) was 728 ± 59 mm, resulting in an integrated crop coefficient (K_c) of 0.88 ± 0.1 for the rice growing season. The K_c value for initial stage was 0.87 ± 0.07, development stage 1.02 ± 0.08, middle stage 1.02 ± 0.08, and late stage 0.77 ± 0.10. The annual mean of inherent water use efficiency (W_{ei}) was 16.4 ±

3.6 gC kg H_2O^{-1} hPa with large interannual variations. In terms of the annual carbon budget, gross primary productivity (*GPP*), respiration of ecosystem (*RE*), and net ecosystem exchange (*NEE*) were 1235 ± 90, 1139 ± 54, and -97 ± 119 gC m^{-2}, respectively. Annually integrated R_n was averaged to be 2567 ± 102 MJ m^{-2} and the energy partitioning in terms of the Bowen ratio (β) was 0.39 ± 0.05. The energy balance ratio (EBR) for an annual budget closure ranged from 0.80 to 0.90. The mean annual internal entropy production (σ) was 12.88 ± 0.35 MJ m^{-2} K^{-1} while that of entropy transfer (*J*) was negative (-11.89 ± 0.36 MJ m^{-2} K^{-1}), indicating the net transfer out of the system into the environment. The time rate of change in system entropy (dS/dt) fluctuated throughout the study period with an average of 1.39 ± 0.30 MJ m^{-2} K^{-1}.

The highlights of this research results are: 1) *ET* was limited not by the limitation of water but by the availability of energy, 2) the variation of K_c is mostly related to the fluctuation of *ET*, 3) low water use efficiency indicates a relatively poor use of water in this agricultural ecosystem, 4) the consistent overproduction of entropy throughout the decadal study period indicates a degradation of this agricultural ecosystem due to human disturbance, and 5) further studies are needed to bridge the quantified biophysical characteristics summarized above with thermodynamic and self-organization indicators tested in this study.

Keywords: sustainability, thermodynamic approach, water use, agricultural ecosystem, eddy covariance technique.
Student Number: 2013-22563.

TABLE OF CONTENTS

LIST OF TABLE

LIST OF FIGURES

1. Background of the Study

1.1 Motivation

From a thermodynamics point of view, any ecosystem in the Earth system is an open system which exchanges energy (incoming solar radiation and outgoing heat irradiation) and matter (water, carbon dioxide, nutrients, organic matter, etc.) with the environment (Jorgensen and Svirezhev, 2004). The other case, an isolated system can only increase its entropy (i.e. a measure of the quality of energy) or there is the depletion of free energy over time (Kleidon, 2009), which can only sustain life for only a limited period of time, less than that required for the onset of isolation to reach thermodynamic equilibrium (i.e. no future change is possible). In other words, an isolated system will die. The openness of an ecosystem is the reason why the system can maintain its life and stay away from thermodynamic equilibrium because, through the openness, the thermodynamic equilibrium state can be avoided by exporting the entropy production (Jorgensen and Svirezhev, 2004).

Agricultural ecosystem is an open system which can be described as the example of the elementary ecosystem under anthropogenic pressure (e.g. management practice) (Svirezhev, 2008). Elementary ecosystem is the area unit of land, covered by some type of vegetation, and upper layer of soil with litter, in which death organic matter (DOM) is decomposed.

These days, agricultural practice is greatly developed with higher resource

intensity and causes environmental impacts. However, food security is not yet established. Agricultural ecosystems globally occupied 38% of the Earth's terrestrial surface, emerging as the largest land use (Ramankutty *et al*., 2008) and the largest consumer (i.e. around 70 %) of all freshwater withdrawals for food production. To meet the world's future food security and sustainability needs, food production must grow substantially to provide a certain level of food demands from population growth. On the other hand, agricultural environmental footprint must shrink dramatically (Foley *et al*., 2011).

An assessment of sustainability is necessary to find out whether the current setting of agricultural management is a proper configuration toward sustainable management particularly of water use. How to describe the current state of an agricultural ecosystem and its dynamic under human intensive management are the necessary steps to be identified in order to develop the necessary index of the system state toward sustainable water use management. Agricultural ecosystem as an open system allows the exchange of energy and matter within the boundary, enabling the system's entropy to remain constant or even decrease (Jorgensen and Svirezhev, 2004). By knowing how to calculate the entropy balance for agricultural ecosystem, the anthropogenic impact can be associated with an increase in the system entropy.

In this research, the assessment of water use (i.e. evapotranspiration (ET), crop coefficient (K_c) and inherent water use efficiency (W_{ei})), carbon and energy

exchange of an agricultural ecosystem was performed by using conventional quantification and then entropy budget assessment was used to identify and describe the dynamic of the current state of agricultural ecosystem.

In this research, the eddy covariance measurement data were used of Haenam KoFlux site (HFK) as a representative of typical managed farmland that is dominant in suburban and rural areas in Korea (Park *et al.,* 2006). HFK is a heterogeneous farmland ecosystem which is assumed to have higher resilience compare with monoculture practice. In Korea, 15.8 billion m^3 or 50% of water resources is used for farming (MAFRA, 2013). The unique characteristic of monsoon climate in Korea provides about 70% of its annual precipitation between June and September, also facing great challenges due to climate change which can be seen in the appearance of repeated flooding and severe drought events in recent years (Kwon *et al*., 2008; Kyoung *et al*., 2011). Korea is also classified as a water-deficient country by the United Nations (UN).

KoFlux, a Korean regional flux monitoring network, has been monitoring CO_2 and water exchange using the eddy covariance technique for major plant functional types in Korea, providing multiyear direct measurement data. Tower flux data from KoFlux sites have been broadly used to conduct researches on the influence of Asian monsoon on carbon and water exchange in forest ecosystem and farmland (e.g. Kang *et al.,* 2009 and 2012; Kwon *et al.,* 2010), remote sensing

application (e.g. Kim *et al*., 2006; Byun *et al*., 2012; Ryu *et al*., 2012) and atmospheric and land surface model development (e.g. Hong *et al.*, 2010; Yuan *et al.*, 2011; Hong *et al.*, 2011; Lee *et al*., *2014*) (see Section 1.3 for detailed documentation).

The expected result based on preliminary analysis indicated the overproduction of entropy in the system, which can trigger the system performance to become weaker (e.g. inefficient water use, lowering *GPP*). Eventually, through the long-term documentation of energy and water use at an agricultural ecosystem, it can give an alternative option of management in HFK in particular as well as the application of the lessons to other ecosystems using the same framework.

1.2 Conceptual Framework

The conceptual framework of this research borrows the complex systems concept from Kay and Boyle (2008) who view ecosystems as coupled ecological-societal systems. The human-constructed societal systems depend on the flows of energy, material, and information from the natural ecological systems to support their processes and structures. These flows, together with the biophysical environment provided by ecological systems, are the context for societal systems. However, the societal systems can also influence the ecological systems when humans change the structures of the ecological systems and when the societal

systems alter the context for the ecological systems. In short, the relationships between ecological and societal systems are 1) ecological systems provide the context of societal systems, 2) the societal systems can alter the structures in ecological systems, and 3) the societal systems can alter the context for self-organizing processes of ecological systems.

This ecological-societal system point of view can help for us to better describing the system, explaining the dynamics, and synthesizing the understanding of the system that we are concern. Applying this to agricultural ecosystem in HFK, the diagram of system boundary was made.

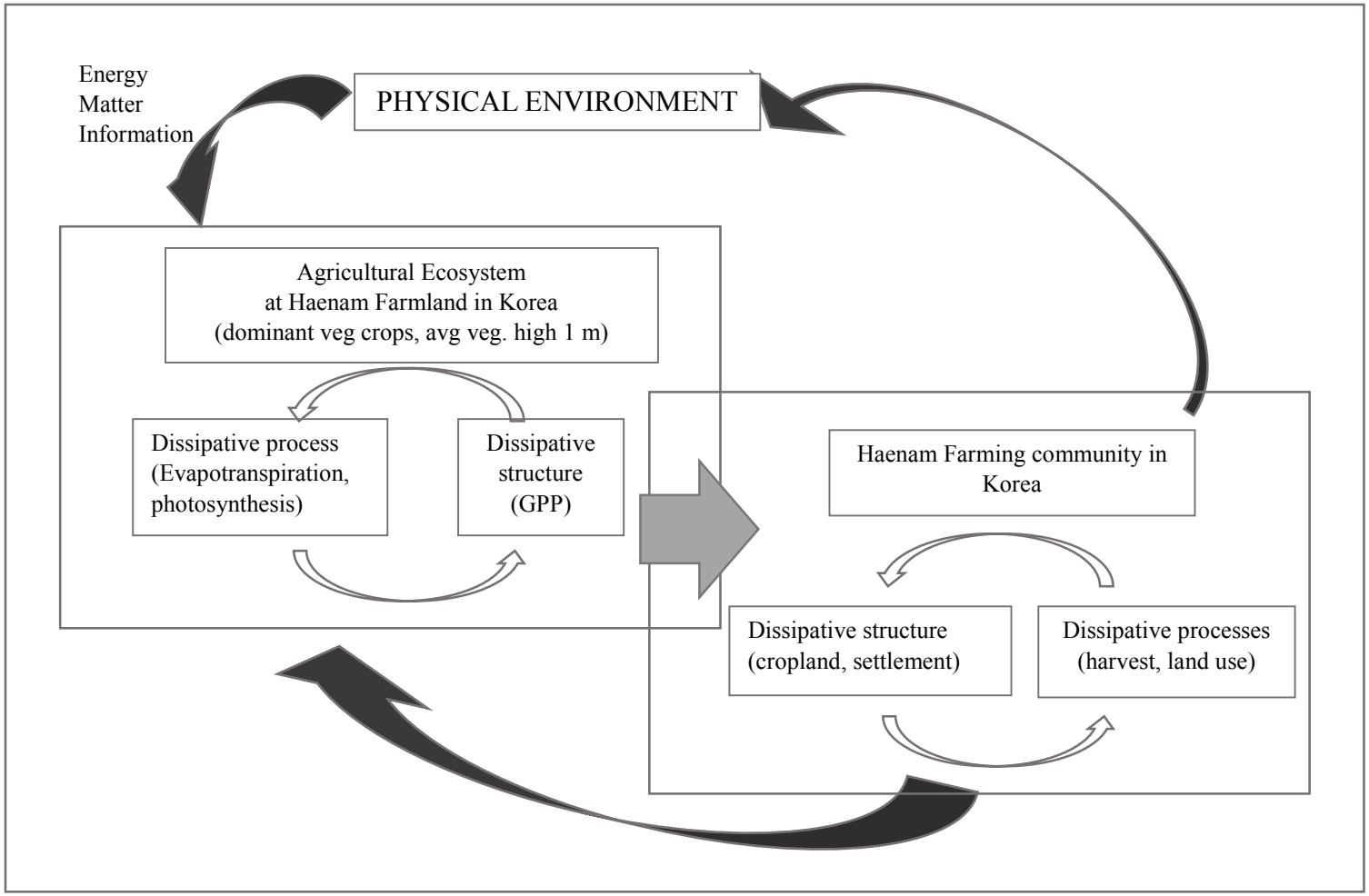

Figure 1 Diagram of system boundary of agricultural ecosystem at Haenam Farmland in Korea (HFK).

1.3 Haenam Farmland in Korea (HFK)

Since the establishment of tower flux measurement at HFK site, a variety of researches have been conducted covering many fields of studies. Reviewing what have been done at HFK would provide better understanding and ideas about the history of HFK site. Most of the researches conducted at HFK are about energy, CO_2 and water exchanges. Lee *et al*. (2003) documented the first result of EC measurement at HFK by highlighting the maintenance of EC system during the early stage of measurement, the documentation of instrumentation, data processing, and the results of preliminary analysis during the first year in 2002. Kwon *et al*. (2009) examined the seasonality of the individual carbon budget components (i.e. *NEE*, *RE*, and *GPP*) and showed that there were distinctive bimodal peaks with a mid-season depression. Furthermore, Kwon *et al*. (2010) assessed the influence of the monsoon season on *NEE* and attributed the re-occurrence of the mid-season depression of *NEE* each year to human disturbance (i.e. land management by rotating two crops) rather than natural disturbance (i.e. monsoon and typhoons).

Among other studies focusing on hydrological cycle, Kang *et al*. (2009) reported the first complete annual ET measurement using eddy covariance technique. The annual *ET* averaged from 2004 to 2006 was about 323 mm which accounted for 41% of annual precipitation (*P*). They also found out that *ET* also showed the mid-season depression mainly due to reduced available energy

associated with summer monsoon and typhoon. Kwon *et al*. (2011) conducted error assessment of climate variable which is used in FAO-56 reference *ET* computation. The estimated radiation, vapor pressure, and wind speed were compared against the observation data in 2008. Despite the differences between the estimated and the observed radiation and wind speed, the comparison of ET_o showed small differences with a mean bias error (MBE) varying from -0.22 to 0.25 mm d^{-1} and a root mean square error (RMSE) varying from 0.06 to 0.73 mm d^{-1}.

In terms of remote sensing application, Ryu *et al.* (2008) evaluated the performance of moderate resolution imaging spectroradiometer (MODIS) over a complex terrain and heterogeneous landscape on clear sky days. They showed that solar radiation was successfully retrieved with a RMSE of ~20 W m^{-2} for both the Terra and Aqua devices over the flat HFK site. The sensitivities of the upward components of the shortwave and longwave radiation components varied with RMSE values to the scale of the spatial heterogeneity. Consequently, the RMSE values of the net radiation ranged from 33 to 61 W m^{-2} for both the devices. Then, Moon *et al*. (2010) analyzed the heterogeneity of HFK using Landsat TM satellite image data. They showed that the characteristic scales of albedo at HFK was approximately 0.3 km. For land surface temperature (LST), the scale of heterogeneity was varying from 0.6 to 1.0 km and there was little seasonal change in the characteristic scales.

Researches on modelling have been conducted also at HFK. Lee *et al*. (2008) used two layer canopy model (mSPA model) to examined the exchange of CO_2 and water vapor over a paddy field in the growing season of 2003 in four different cases. The results of diurnal variations of turbulence fluxes agreed well with those of observation under the conditions of near maximum LAI, large root biomass and moderate vapor pressure deficit (*VPD*). Common Land Model (CLM) was also tested to understand the model performance for water and energy fluxes during the growing season in Korea (Choi *et al*., 2010). The simulated soil moisture was relatively lower than that of the observed. The simulated net radiation showed a good agreement with the observed (RMSE of 41 W m^{-2}). However, relatively large discrepancies between the simulation and the observation were found in sensible heat flux (RMSE of 66 W m^{-2}) and latent heat flux (RMSE of 60 W m^{-2}). Soil moisture was more receptive to land cover and soil texture parameterizations, compared to soil temperature and turbulent fluxes. The initial performance of CLM suggests usefulness in a data-limited heterogeneous farmland in Korea. Other studies were conducted to model spatial and temporal variations in planetary boundary layer (PBL) height over the Korean Peninsula (Lee *et al.,* 2013). Measurement data at HFK (i.e. latent heat flux (*LE*), sensible heat flux (*H*), and wind speed (*ws*)) were used to identify the characteristic of PBL during the specific periods of plant growth and photosynthetic activity.

2. Material and Method

2.1 Site Description

HFK site is located in southwestern end of the Korean Peninsula (34.55ºN, 126.57ºE, 13.74 m above mean sea level) with relatively flat terrain except the southeast section with a slope of about 4º (http://asiaflux.net/index.php?page_id=60). The land cover around the study site has been the mixture of rice paddies and various agricultural crops. Within the first 300 m around the tower, the major vegetation included seasonally cultivated crops such as beans, sweet potatoes, Indian millet, and sesame. Beyond this area, rice paddies prevailed in the south and the west. Also, scattered residential areas, roads and isolated forests coexisted.

Figure 2 HFK location map.

The mean canopy height of dominant species was approximately 1 m. For the past 30 years, mean annual air temperature was 13.3ºC with the maximum and minimum of 18.6ºC and 8.6ºC, respectively (Lee *et al*., 2003). The climate at HFK is typical of moist subtropical mid-latitude (i.e. hot, humid summer and cool, dry winter) and the soil type varies from silt loam to loam (sand 38.5%, clay 30.0%) (Lee *et al.,* 2008). The growing season period at HFK was divided into the spring barley growing season from April to May, and the rice-paddy growing season from Jun to October, following Kwon *et al*. (2009).

2.2 Field Measurement and Flux Data Processing

Flux measurement using eddy covariance technique has been conducted since July 2002 until now. The data from 2003 to 2012 (excluding the year 2005 and 2007 with > 50% gaps) were used for this study. The main eddy covariance system was consisted of a three-dimensional sonic anemometer (CSAT3, Campbell Scientific Inc, Logan, UT) and an open-path H_2O/CO_2 gas analyzer (LI7500, LICOR, Lincoln, NE), which were installed at 20.8 m above the ground. Radiation components were measured using a 4-component net radiometer (Model CNR1, Kipp & Zonen, Delft, the Netherlands) at 15m above ground. Precipitation was obtained from the on-site automated weather station operated by Korean Meteorological Administration. Half-hour eddy covariance and the associated

statistics were calculated online from 10 Hz raw data, and other meteorological variables (e.g. net radiation, air temperature, humidity, soil temperature, soil water content, and precipitation) were measured and averaged every 30 minutes.

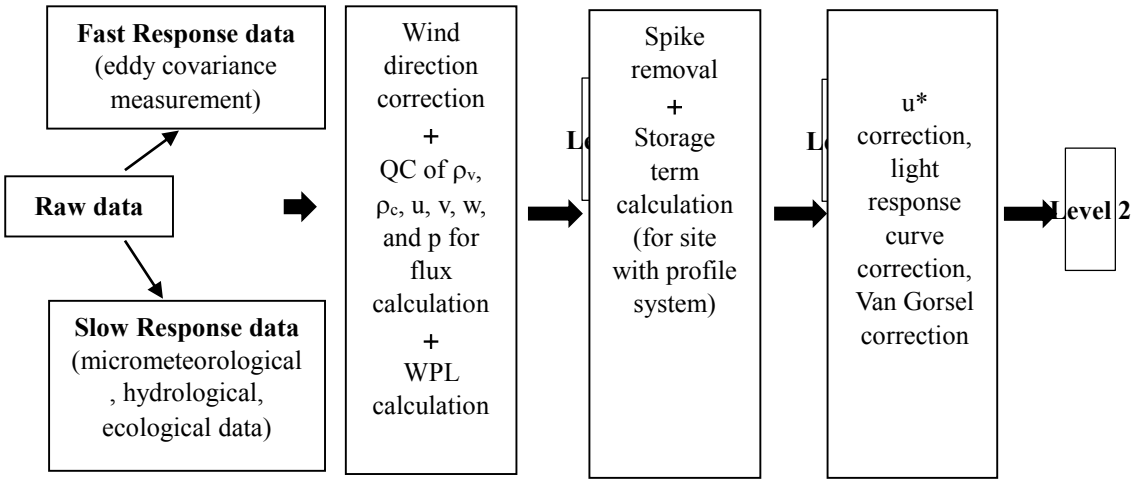

Figure 3 Data processing procedures.

The eddy covariance data were post-processed, quality-controlled, and gap-filled using the standardized KoFlux protocol which includes coordinate rotation, density correction, spike detection, storage correction, nighttime correction, gap-filling, and the estimation of *GPP* and *RE*, which is similar to the FLUXNET data processing. For gap-filling method, u* correction, light response curve, and the Van Gorsel methods were applied and then the average of those three method was used for further analysis.

2.3 Theoretical Background

2.3.1 Energy and Entropy Budget

Energy balance equation of the system is written as :

$$R_{net} = (1 - \alpha_s)R_{s\downarrow} + (1 - \alpha_l)R_{l\downarrow} + R_{l\uparrow} = -(LE + H) + dG/dt \quad (1)$$

where R_{net}, $R_{s\downarrow}$, $R_{l\downarrow}$, and $R_{l\uparrow}$ are the net, incoming shortwave, incoming and outgoing longwave radiation fluxes (W m^{-2}). The Bowen ratio (β) calculated as $\beta = H/LE$ and Energy Balance Ratio calculated as EBR $= R_n/(H + LE)$ (2).

Entropy balance equation in an open system derived based on energy balance equation following Kleidon (2010 and 2012) as:

$$dS/dt = \sigma + J \quad (3)$$

where S is the system entropy (MJ m^{-2} K^{-1}), σ is the time rate of total entropy production within the system (W m^{-2} K^{-1}), and J is the time rate of total entropy transfer from and to the system (W m^{-2} K^{-1}). The total entropy production (σ) consists of the entropy production by energy dissipation of the absorbed downward shortwave radiation ($R_s\downarrow$) and absorbed downward longwave radiation ($R_l\downarrow$), so that:

$$\sigma = \sigma_{Rs} + \sigma_{Rl} \quad (4)$$

$$\sigma_{Rs} = (1 - \alpha_s)R_{s\downarrow}(1/T_{sys} - 1/T_{sun}) \quad (5)$$

$$\sigma_{Rl} = (1 - \alpha_l)R_{l\downarrow}(1/T_{sys} - 1/T_{atm}) \quad (6)$$

where T_{sun} is the temperature of the sun assumed to be constant at 5780 K, T_{sys} and T_{atm} are the temperature of the system and atmosphere respectively (K) which are estimated using observed $R_{l\uparrow}$ and $R_{l\downarrow}$ and Stefan-Boltzmann equation (i.e. $R_l = \varepsilon \varsigma T^4$, where ς is the Stefan-Boltzmann constant (5.67×10^{-8} W m^{-2} K^{-4}) and ε is the emissivity of the object that is ≈ 0.98 for plant (Humes *et al*., 1994) and ≈ 0.85 for atmosphere (Campbell and Norman, 1998).

On the other hand, the entropy transfers associated with energy exchange is defined as:

$$J = J_{Rsnet} + J_{Rlnet} + J_{LE} + J_H \tag{7}$$

$$J_{Rsnet} = {R_{snet}}/{T_{sun}}\,,\ J_{Rlnet} = J_{Rl\uparrow} + J_{Rl\downarrow}\,,\ J_{Rl\uparrow} = {R_{l\uparrow}}/{T_{sys}}\,, \tag{8}$$

$$J_{Rl\downarrow} = {(1-\alpha)R_{l\downarrow}}/{T_{atm}}\,,\ J_{LE} = {LE}/{T_{sys}}\,,\ J_H = {H}/{T_{sys}} \tag{9}$$

where J_{Rsnet}, J_{Rlnet}, $J_{Rl\downarrow}$, $J_{Rl\uparrow}$, J_{LE}, and J_H are the entropy transfers associated with R_{snet}, $R_{l\downarrow}$, $R_{l\uparrow}$, LE, and H, respectively (W m^{-2} K^{-1}).

The function of Entropy pump is sucking the entire entropy out of ecosystems so that there may be no overproduction of entropy. Consequently, the system can exist during a sufficiently long time period and it will be clearer if the process is considered as a cyclic process (Jorgensen and Svirezhev, 2000).

2.3.2 Actual Evapotranspiration

Evapotranspiration on a global average is accounts for 60% of the annual precipitation falling over the land that return to the atmosphere. Accurate quantification of *ET* is crucial in water allocation, irrigation management, evaluating the effects of changing land use on water yield, environmental assessment, and development of best management practices to protect surface and ground water quantity and quality. In this research *ET* was measured using Eddy Covariance technique.

2.3.3 The Budyko Curve

Budyko (1974) assumed that actual evapotranspiration (*ET*) is controlled by both water and energy availabilities and at the annual time scale, the water availability is the amount of annual precipitation (*P*) and the energy availability can be measured by the potential *ET*. The Budyko framework reduces climate to a radiative dryness index ($DI = {ET_p}/{P}$, where ET_p is potential evapotranspiration and the surface water balance to an evaporative index ($EI = {ET}/{P}$) (Williams *et.al*., 2012). *DI* represents the ratio of demand (ET_p) to supply (*P*) for which large values (>1) represent dry/nonhumid conditions under which the rate of *ET* is controlled by the amount of *P* regardless how high ET_p is. On the other hand, small values (<1) represent wet/hummid conditions under which *ET* is limited by ET_p so that *ET*

approaches ET_p and will not increase with P, or the changes in ET are controlled by those in ET_p rather than P. In other words, in dry/non-hummid conditions, changes in ET are dominated by changes in P rather than in ET_p (i.e. water limited). In wet/hummid regions, changes in ET are controlled by changes in ET_p rather than in P (i.e. energy limited) (Yang *et.al*., 2006).

EI is the fraction of available water consumed by the ET process and the residual (1- ET/P) can be inferred as the fraction consumed by runoff or deep drainage (Q) assuming no change in local storage. High value of ET/P represents low run off ratio which also means water loss from ET is significant and vice versa.

Fundamental bounds of the Budyko hypothesis are: 1) the demand limit states that actual ET cannot exceed potential ET_p and traces a 1:1 line coresponding to ET/ET_p =1, 2) the supply limit states that ET cannot exceed water supply, requiring $EI \leq 1$, except where run on or phreatic water sources offer sizable contributions.

Budyko curve is calculated as such [Budyko, 1974]:

$$\frac{ET}{P} = \left(\frac{ET_p}{P}\tanh\left(\frac{P}{ET_p}\right)\left[1 - exp\left(-\frac{ETp}{P}\right)\right]\right)^{0.5} \quad (10)$$

ET_p is firstly introduced by Penman and defined as the amount of water transpired in a given time by a short green crop, completely shading the ground, of uniform height and with adequate water status in the soil profile.

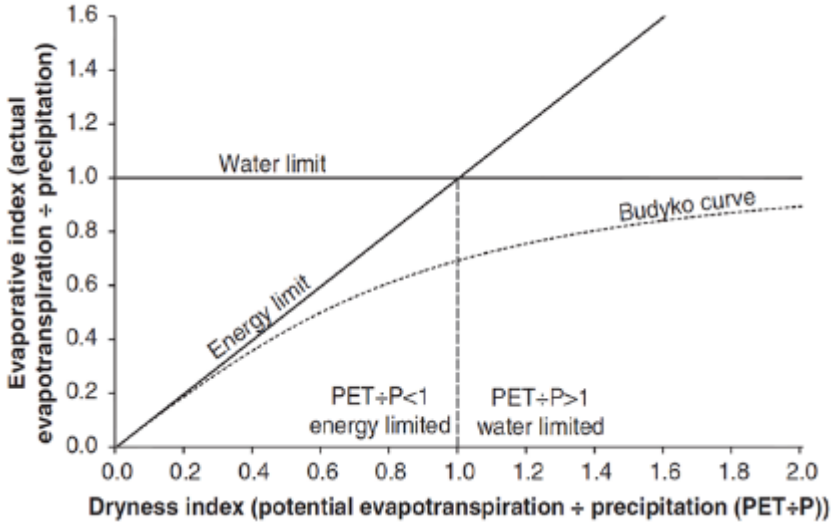

Figure 4 Budyko curve (Jones *et al.*, 2012).

Here, ET_p was calculated on the equation proposed by Priestley and Taylor (1972) which is used when the surface areas generally were wet (i.e. the reqired condition for ET_p).

$$ET_p = \alpha \frac{\Delta}{\Delta+\gamma} \frac{(Rn-G)}{\lambda} \quad , \qquad (11)$$

where ET_p is in mm day^{-1}; R_n is daily net radiation (MJ m^{-2} day^{-1}); G is soil heat density at the soil surface (MJ m^{-2} day^{-1}); Δ is Δ is slope of the vapor pressure-temperature curve (kPa °C^{-1}); γ is psychrometric constant (kPa °C^{-1}); λ is the latent heat of vaporization (2.45 MJ kg^{-1}); and α (=1.26) is the *Priestley-Taylor* coefficient (accounting for effect of advection and large scale entrainment) which explained by Lhomme (1996) for the *ET* from a horizontally uniform saturated surface that closely resembles a surface of well-watered short grasses under humid condition.

2.3.4 Reference Evapotranspiration

Reference *ET* (ET_o) is defined as the rate of *ET* from hypothetically reference surface (assumed crop height of 0.12 m, fixed surface resistance of 70 sm^{-1} and an albedo of 0.23) which is closely resembling the *ET* from an extensive surface of green grass of uniform height, actively growing, well watered and completely shading ground (Allen *et al*., 1998). ET_o was calculated at HFK using FAO-56 Penman-Monteith equation (Allen *et al.,* 1998):

$$ET_o = \frac{0.408\,\Delta\,(Rn-G)+\gamma\left(\frac{Cn}{T+273}\right)U_2(e_s-e_a)}{\Delta+\gamma(1+CdU_2)}, \qquad (12)$$

where R_n is daily net radiation (MJ m^{-2}); G is soil heat density at the soil surface (MJ m^{-2}); Δ is slope of the vapor pressure-temperature curve (kPa $°C^{-1}$); γ is psychrometric constant (kPa $°C^{-1}$); T is mean daily temperature (°C); U_2 is mean daily wind speed at 2 m (m s^{-1}); e_s = mean saturation vapor pressure (kPa); e_a = mean actual vapor pressure (kPa); C_n is numerator constant for reference type and calculation time step which is 900 for short reference; C_d is denominator constant for reference type and calculation time step which is 0.34 for short reference.

The wind speed at 2 meter height (U_2) was calculated using wind speed profile equation (Rosenberg *et al.,* 1983):

$$\frac{U_2}{U_1} = \frac{\ln(z_2-d)-\ln(z_o)}{\ln(z_1-d)-\ln(z_o)}, \qquad (13)$$

where U_z is actual measurement of wind speed at certain high above ground surface

(m s^{-1}); U_2 are wind speed at 2 m above ground surface (m s^{-1}), z_z and z_2 are the measurement height and d is zero place displacement and z_z is roughness length. The available energy component $(Rn - G)$ was replaced by $(H + LE)$ which were measured together with other components (i.e. $(e_s - e_a)$) using eddy covariance system measurement.

2.3.5 Crop Coefficient

Crop coefficient (K_c) defined as the rates of *ET* from the various crops related to those from the reference surface (ET_o). It represents the crop specific water use (Kashyap and Panda, 2001) or the effect of the crop characteristics on crop water requirement (Doorenbos and Pruitt, 1977). K_c is calculated as the ratio of ET to ET_o, which can be used with ET_o to estimate specific crop *ET* if there is no actual measurement (Allen *et al*., 1998). The crop type, variety and development stage should be considered when assessing the *ET* from crops grown in large, well-managed fields. Differences in resistance to transpiration, crop height, crop roughness, reflection, ground cover and crop rooting characteristics result in different *ET* levels in different types of crops under identical environmental conditions. In this research, *ET* was measured directly by eddy covariance measurement.

2.3.6 Water Use Efficiency

Water use efficiency is defined as the amount/rate of carbon gained per unit of water loss (Beer *et al*., 2009; Vickers *et al*., 2012; Keenan *et al*., 2013). For many years, considerable research of water use efficiency are actively conducted and published which cover leaf (Jones and Rawson, 1979; Polley *et al*., 1996) to ecosystem scale (Law *et al*., 2002; Lloyd *et al*., 2002; Reichstein *et al*., 2002; Kuglitsch *et al*., 2008) for different types of climate conditions (Tian *et al*., 2011; Brummer *et al*., 2012) and vegetation (Yu *et al*., 2007; Hu *et al*., 2008; Wolf *et al.,* 2013; Xiao *et al*., 2013). Various methods to calculate water use efficiency were also developed to capture vegetation response toward the environmental change by using the Bowen ratio (Baldocchi *et al.*, 1985), isotope (Farquhar and Richards, 1984), modeling (Wang *et al*., 2004) as well as eddy covariance (Law *et al*., 2002; Beer *et al*., 2007; Kuglitsch *et al*., 2008).

Beer *et al*. (2009) which proposed inherent water use efficiency (W_{ei}) to calculate water use efficiency at ecosystem level. For whole plants or ecosystems, W_{ei} can be calculated in a similar fashion as for leaves as:

$$W_{ei} = \frac{GEP}{E_e(1-\phi w)} \qquad (14)$$

where E_e is ecosystem evapotranspiration, and ϕ_w represents the fraction of non-transpiratory water loss.

Transpiration and thus W_{ei} are functions of evaporative demand and the latter

is used when comparing water-use efficiency between different species or meteorological conditions. At the ecosystem level, W_{ei} can be approximated using eddy-covariance flux measurement, as the ratio between *GEP* and canopy conductance by approximating the vapor pressure difference by atmospheric *VPD* under the assumption that (1) vapor pressure difference between the leaf and the atmosphere can be approximated by measured atmospheric evaporative demand (*VPD*), assuming equal temperatures of leaves and atmosphere, (2) aero-dynamic resistance between the canopy and the reference-height for the flux can be neglected, (3) under dry conditions, with no recent precipitation events, measured water vapor fluxes are equivalent to transpiration (Keenan *et al*.,2013) and (4) by approximating carbon assimilation *A* and transpiration *E* by *GPP* and *ET* inferred from flux tower observations of *NEE* and latent energy during dry days (Beer *et al*., 2009). Then W_{ei} is formulated as:

$$\mathrm{W_{ei}} = \frac{\mathrm{GPP}}{ET}.\mathrm{VPD} \qquad (15)$$

Here, data from rainy days as well as the two post-rainfall days were excluded from analysis following Beer *et al*. (2009) and Keenan *et al*. (2013) to focus on transpiration rather than bare soil evaporation and interception of the measured total evapotranspiration. The study of Beer *et al*. (2009) on ecosystem level water use efficiency (W_{ei}) demonstrated the suitability of using flux measurement data from eddy covariance technique to derive proxies of intrinsic water use efficiency at

ecosystem level and showed the increase in W_{ei} during a short term drought period. Keenan *et al*. (2013) also used W_{ei} to show the increase in W_{ei} as the increase in atmospheric CO_2 in temperate and boreal forests of the Northern Hemisphere by using direct and continuous long-term measurement. Other research using W_{ei} related to drought by Vickers *et al.* (2012) showed that W_{ei} in two pine forests increased during the seasonal drought.

2.3.7 Footprint Analysis

Flux footprint is important to estimate the location and relative importance of passive scalar source influencing flux measurement at a given height (Kljun *et al*., 2004) especially at heterogeneous sites where the horizontal and vertical variability of measured fluxes of surface-atmosphere exchange must be accounted for (Schmid, 2002). The spatial variability of the source strength is usually controlled by the surface vegetation characteristics and soil conditions (Chen *et al*., 2012) and assumed that vegetation density variability is significantly correlated with the source of flux strength (Kim *et al*., 2006).

Recently, a number of footprint models have been presented using analytical, stochastic, or numerical approaches in Eulerian or Lagrangian frameworks which were reviewed in detail by Schmid (2002) in terms of model strength and weakness and the limitation of footprint concept its self.

Here, footprint analysis is calculated based on the footprint model of Hsieh *et al*. (2000) which is an approximated analytical model developed to estimate scalar flux footprint in thermally stratified atmospheric surface layer (ASL) flows. The proposed model was based on a combination of Lagrangian stochastic dispersion model results and dimensional analysis. It uses a model by Thomson (1987) with turbulence considered in the vertical only to estimate footprint according to a crosswind integrated version over a range of stabilities, roughness lengths and measurement height. The main advantage of this model is its ability to analytically relate atmospheric stability, measurement height, and surface roughness length to flux and footprint. The flux can be estimated by:

$$F(x, z_m) / S_0 = exp\left(\frac{-1}{k^2 x} D z_u^p |L|^{1-P}\right) \quad (16)$$

and the footprint by

$$f(x, z_m) = \frac{-1}{k^2 x} D z_u^p |L|^{1-P} exp\left(\frac{-1}{k^2 x} D z_u^p |L|^{1-P}\right) \quad (17)$$

where F is the scalar flux, f is the footprint, z_m is the measurement height, x is the mean wind direction is along the horizontal coordinate, S_0 is the source of strength (g m^{-2} s^{-1}), L is the Obukhov length, D and P are similarity constants. The input data for the model are mean wind speed (m s^{-1}), standard deviation of lateral wind speed (m s^{-1}), air temperature (°C), sensible heat flux (W m^{-2}), friction velocity (m s^{-1}), wind direction (°), latent heat flux (W m^{-2}), and CO_2 flux (mg m^{-2} s^{-1}).

3. Results and Discussion

3.1 Climate Conditions

3.1.1 Precipitation (*P*)

P provides natural source of water for agricultural ecosystem at HFK. The average of annual *P* was 1454 ± 188 mm. *P* showed decreasing and then increasing pattern with highest *P* happen in 2003 (279 mm higher than average) followed by 2012 (145 mm higher than average) and lowest *P* happen in year 2008 (348 mm lower than average) followed by year 2009 (181 mm lower than average). *P* showed decreasing then increasing pattern during the study period with three consecutive years below the average (2006-2009), and very high *P* only occurred at the beginning of the observation year (2003).

The study by Song *et al*. (2014) in regional scale included HFK showed the anomaly of annual *P* from 2002 to 2009 and the period that was selected as a benchmark of abnormal year, were 2003 as an abnormally large *P* and 2008 as an abnormally small *P*. Compared with 30-years climate normal (1981-2010), average annual *P* for 8 years is 100 mm higher.

Table 1. Annual and seasonal *P*

Seasonal	2003	2004	2006	2008	2009	2010	2011	2012	avg	std
winter	110	99	59	92	107	235	85	157	**118**	**51**
spring	511	223	386	313	291	440	271	367	**350**	**89**
summer	801	932	755	594	719	639	852	779	**759**	**103**

fall	312	334	151	108	158	185	279	422	**243**	**102**
annual	**1734**	**1587**	**1350**	**1107**	**1273**	**1498**	**1486**	**1725**	**1470**	**204**

Seasonally, more than 50 % (i.e. 53 ± 5 % in average) of *P* came from summer, mostly was occurred from July to August. In relation with the occurring of monsoon (i.e. happen in summer season in Korea which is indicated with intensive rainy periods), positive anomaly in summer season happen in 2003, 2004, 2011 and 2012 with the highest anomaly observed in 2004. While, negative anomaly of *P* (i.e. below annual averages) occurred in 2006, 2008, 2009, 2010 and 2011 with the highest negative anomaly happen in 2008.

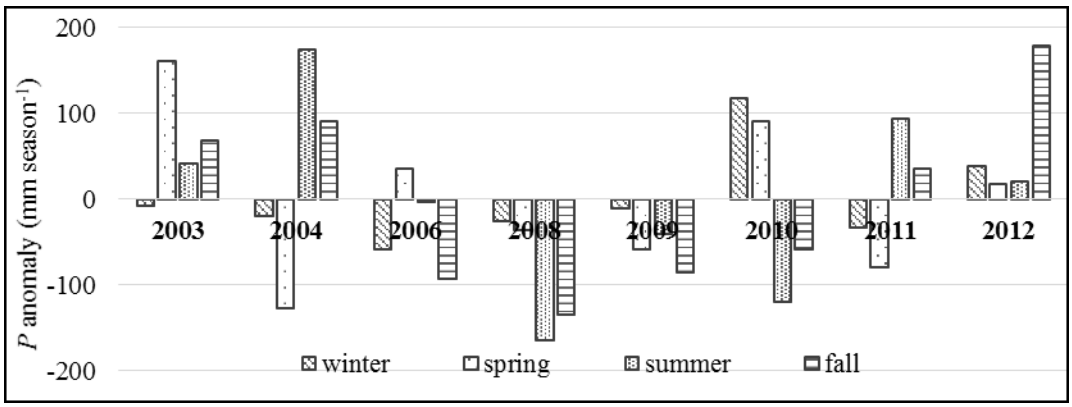

Figure 5 Anomaly of amount of *P* (baseline 2003-2012).

Year with most rainy days happen in 2003 then 2010 while 2012 had the lowest rainy days. Most of the time the highest number of rainy days is occurred at summer with the existence of monsoon especially for year 2009 and 2011 which reach ± 35 % from annual rainy days. In year 2004 and 2008, spring and summer

season had the equal number of rainy days.

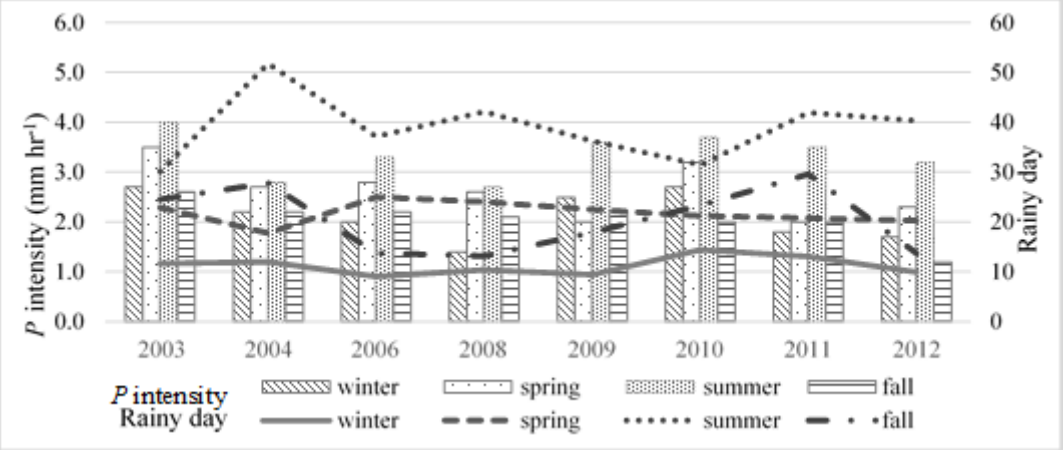

Figure 6 Rainy days and *P* intensity.

As the result of monsoon event during summer, *P* intensity at summer was much higher compared with other season. In contrary with the number of rainy days in summer, year 2004 and 2008 has high intensity of rain in summer compared with other years. There is no extreme event such as typhoon that occurred at HFK that caused a huge amount of *P*. However, typhoon event (i.e. typhoon bolaven) that passed by area closed to HFK in 2012, resulted in very strong wind speed (51.8 m^{-2}) which could affected agricultural ecosystem there.

3.1.2 Downward Shortwave Radiation ($R_s\downarrow$)

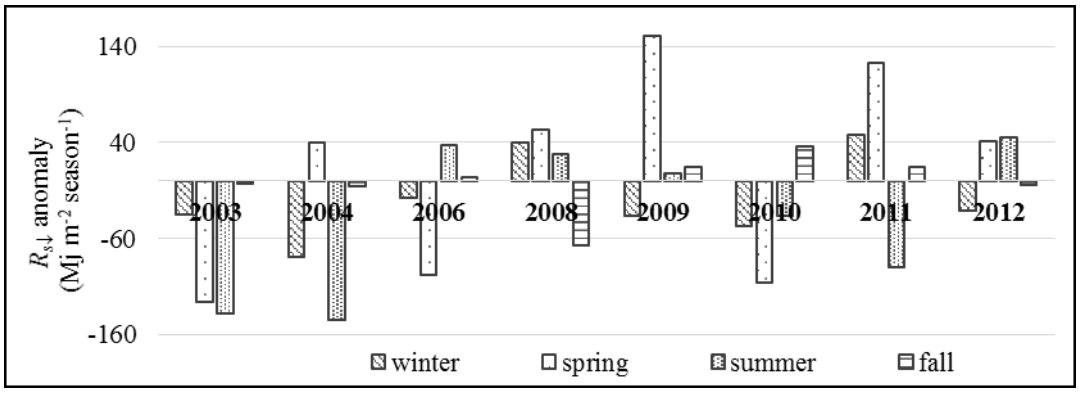

Figure 5 Anomaly of $R_s\downarrow$ (baseline 2003-2012).

The mean value of integrated annual downward shortwave radiation ($R_s\downarrow$) was 5025 ± 154 MJ m^{-2}. $R_s\downarrow$ showed fluctuation pattern with 2003 received lowest $R_s\downarrow$ (4724 MJ m^{-2}) which related with highest P in that year and 2004 received highest $R_s\downarrow$ even though the amount of P was not low. In the year with low amount of P (2006-2009), $R_s\downarrow$ observed higher than the mean integrated value. In 2012, even though P was high, annual and seasonal $R_s\downarrow$ showed slightly above the average.

Due to monsoon period in the summer, $R_s\downarrow$ in the summer was lower than in the spring time. Interannual variation of seasonal $R_s\downarrow$ generally showed gradually increasing pattern throughout the observation years. High negative anomaly during summer observed in the early observation years and then gradually increased and become higher than the average except in 2010 and 2011. $R_s\downarrow$ value especially in the summer is highly related with P which showed the opposite pattern. The

fluctuation of $R_s\downarrow$ which is the main energy resource of *ET* eventually is become a limiting factor for *ET* when the available of water is not limited.

3.1.3 Air Temperature (T_a)

The average of annual temperature (T_a) during the measurement period (2003-2012) was 13.6˚C with minor year to year variation with difference less than 0.5˚C. Compared with 30-year climate normal (1981-2010) for HFK site, mean annual T_a for 8 years showed 0.2 ˚C higher than 30-years (1981-2010) climate normal (13.4˚C). Seasonal mean T_a ranged from 2.2 (±0.1) in winter to 24 (±0.7) during summer, highest year to year variation happen in the summer.

Table 2. Annual and seasonal air temperature (T_a) in °C

	2003	**2004**	**2006**	**2008**	**2009**	**2010**	**2011**	**2012**	**Avg**	**std**
winter	2.3	2.3	2.2	2.3	2.3	2.2	2.2	2.1	**2.2**	**0.1**
spring	12.6	12.1	11.5	12.3	12.5	11.3	11.0	12.2	**11.9**	**0.5**
summer	22.7	24.1	23.6	23.9	23.6	24.8	24.3	24.9	**24.0**	**0.7**
fall	16.0	15.7	15.6	16.0	15.8	15.7	16.5	14.9	**15.8**	**0.4**
Annual	**13.4**	**13.6**	**13.3**	**13.6**	**13.5**	**13.5**	**13.5**	**13.5**	**13.5**	**0.1**

T_a showed gradually increasing pattern that showed in its anomaly. Seasonally, the lowest anomaly showed summer the beginning of observation years and gradually increase for the rest of the years then reached highest anomaly at the end of observation years especially in summer. The increase of T_a can increase the

rate of *ET* by giving a warm environmental condition.

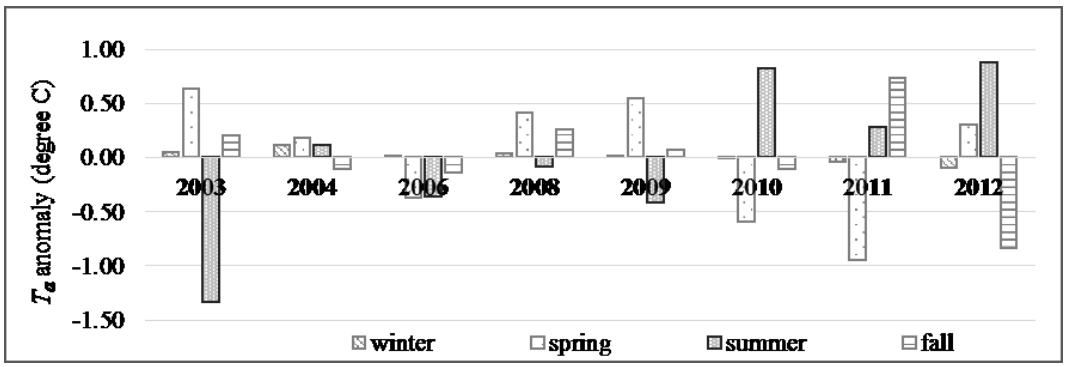

Figure 6 Anomaly of T_a (baseline 2003-2012).

3.1.4 Relative Humidity (*H*)

Relative humidity (*H*) is the measure of vapor amount in the air where 100% corresponds to saturation and lower percentages indicate drier conditions. *H* during observation years varied with the season and showed small inter-annual variation. Generally, summer season for all years has the highest *H* which was ranged between 74 to 82% followed by fall season (72 ± 2.6%). While in winter which is typically dry, *H* was 67 ± 0.2%.

Table 3. Annual and seasonal relative humidity

	2003	2004	2006	2008	2009	2010	2011	2012	Avg	Std
winter	67	67	67	67	67	67	67	68	**67**	**0.2**
spring	68	65	72	70	66	69	68	69	**68**	**2.0**
summer	82	74	82	81	81	81	82	81	**80**	**2.6**
fall	72	66	74	74	73	72	74	74	**72**	**2.6**
Avg	**72**	**68**	**74**	**73**	**72**	**72**	**73**	**73**	**72**	**1.8**

3.1.5 Vapor Pressure Deficit (*VPD*)

Vapor pressure deficit is the difference between saturation vapor pressure and actual vapor pressure ($e_s - e_d$). Annual daytime vapor pressure deficit (*VPD*) average value was 6.9 hPa with coefficient of variation was 12%. Interannual variation showed fluctuation pattern in the beginning (from 2003 to 2009) and then decreased in year 2010 and stabilized for the rest of the years. Seasonal *VPD* showed that summer and fall season had big contribution to annual daytime *VPD*.

The interannual fluctuation of daytime *VPD* is showed in the anomaly figure of daytime *VPD*. It clearly showed the changed from all years for all seasons. In the beginning, 2004 had higher value above the average and then drastically decreased in 2006 for all season then gradually increased in 2008. While in 2009, dramatically increased in daytime *VPD* only observed in spring and fall but other seasons were decreased. For the rest of the years, daytime *VPD* fluctuated below the average.

Table 4 Annual and seasonal Vapor Pressure Deficit

	2003	**2004**	**2006**	**2008**	**2009**	**2010**	**2011**	**2012**	**Avg**	**std**
winter	4.0	4.9	3.9	4.0	4.0	3.3	3.2	2.8	**3.7**	**0.6**
spring	6.6	7.5	5.6	7.2	8.5	5.8	6.0	6.2	**6.7**	**0.9**
summer	6.9	11.1	8.7	8.8	8.5	8.1	7.2	8.3	**8.4**	**1.2**
fall	8.3	10.7	9.1	9.2	9.5	7.8	8.1	7.3	**8.7**	**1.0**
Annual	**6.4**	**8.5**	**6.8**	**7.3**	**7.6**	**6.3**	**6.1**	**6.2**	**6.9**	**0.8**

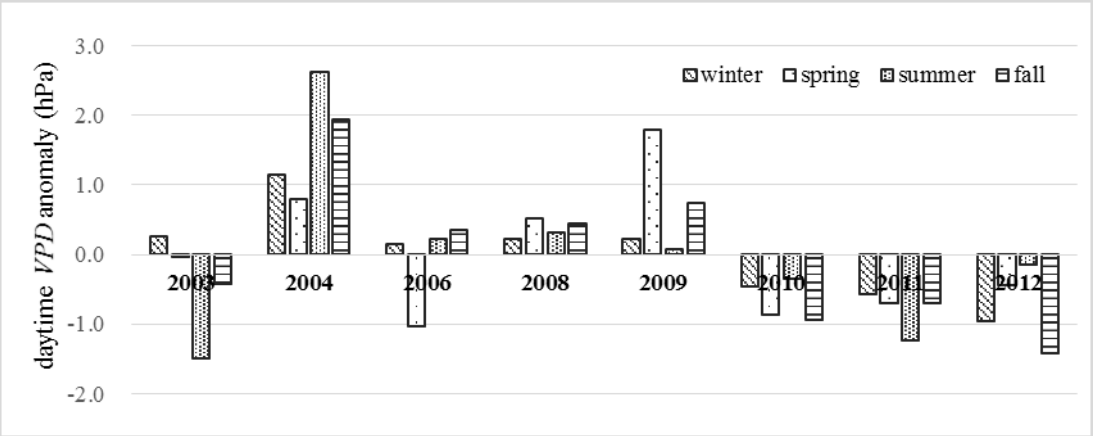

Figure 7 Anomaly of daytime *VPD* (baseline 2003-2012).

3.1.6 Wind

Mean annual wind speed (W_s) during observation years showed small fluctuation which were range from 2.4 to 2.7 m s^{-1}. Seasonally, wind speed was higher during spring and summer and lower during winter and fall. This possible because the present of typhoon which regularly happen in this area. The wind speed during the observation period was higher compared with 30 years climate normal.

Table 5. Annual and seasonal W_s (m s^{-1})

Season	2003	2004	2006	2008	2009	2010	2011	2012	Avg	std
winter	2.3	2.3	2.3	2.3	2.3	2.4	2.3	2.3	**2.3**	**0.0**
spring	2.9	2.8	3.0	2.7	2.9	3.1	2.8	3.1	**2.9**	**0.1**
summer	2.9	2.8	2.6	2.8	2.9	2.7	3.0	3.1	**2.8**	**0.2**
fall	2.1	2.2	1.9	1.8	2.0	2.2	2.1	2.2	**2.1**	**0.1**
annual	**2.6**	**2.5**	**2.4**	**2.4**	**2.5**	**2.6**	**2.6**	**2.7**	**2.5**	**0.1**

3.1.7 Soil Water Content (*SWC*)

Soil water content (*SWC*) can help to explain many processes in the hydrological cycle, which can become a driving factor in the partitioning of infiltration and runoff as well as long-term water storage operated as a feedback mechanism for atmospheric processes. *SWC* can vary significantly among several locations which are near to each other and apparently similar. However, understanding the seasonal condition of *SWC* is important especially for agricultural ecosystem where the source of water is not only from *P*.

Table 6. *SWC* (% volume water) average from May to September

Month	2003	2004	2006	2008	2009	2010	2011	2012
May	0.33	0.34	0.33	0.27	0.26	0.29	0.30	0.24
Jun	0.33	0.32	0.36	0.30	0.19	0.22	0.25	0.18
Jul	0.39	0.36	0.38	0.26	0.30	0.29	0.27	0.29
Aug	0.35	-	0.35	0.20	0.25	0.29	0.29	0.24
Sep	0.35	0.35	0.35	0.20	0.19	-	0.26	0.30
avg	**0.35**	**0.34**	**0.35**	**0.24**	**0.24**	**0.27**	**0.28**	**0.25**
std	**0.02**	**0.02**	**0.01**	**0.04**	**0.04**	**0.03**	**0.02**	**0.04**

Based on *P*, mostly, huge amount of *P* was due to monsoon in summer which affected in increasing *SWC* during that period. *SWC* from May to September for each year was averaged and the range was from 0.24 to 0.35 % of volume water. 2008 and 2009 where *P* were lowest also showed low *SWC* during those periods. Year 2003, which showed high *P* also demonstrated high *SWC* for most of the time. However, for year to year variation, it showed *SWC* was decreasing.

3.2 Footprint Analysis

Heterogeneity of the surface, where EC measurement is conducted, was one of the main issue in flux measurement using EC technic. Over a heterogeneous surface, the measured signal by the turbulent flux sensor depends on which part of the surface has the strongest influence on the sensor and also on the location and size of the footprint (Schmid, 2002). Moon *et al.* (2007) quantified the spatial heterogeneity of the land surface temperature and albedo for HFK and found out that HFK scales of albedo was 0.3 km and scale for land surface temperature was 0.6 to 1.0 km which showed the heterogeneity of HFK.

Footprint models are used as a diagnostic tool to quantify the representativeness of tower flux measurements for selected sites. Recently, long-term patterns of source contributions provide essential information about the vegetation especially over heterogeneous landscapes which can be combined with vegetation characteristic from satellite image (Kim *et al*., 2006).

Footprint analysis by Hsieh (2000) based on Schmid (2002) had good agreement with other model (i.e. Horst and Weil analytic model) in near-neutral conditions, and agreement of the peak footprint location within an order of magnitude of x for unstable and stable conditions. Only vertical turbulence is considered by this method to estimate the footprint according to a crosswind over a range of stabilities, roughness lengths, and measurement heights. That footprint

model was used in this research to observe annual and seasonal pattern of footprint of the agricultural ecosystem at HFK. Footprint analysis was used to figure out the contrasting results between those years were come from the same source or the majority was same or from very different source. Agricultural ecosystem at HFK, as a typical farmland in Korea has characteristic of heterogeneity both spatial and temporal. So that, possibility of different source of fluxes or energy as well as entropy is need to be considered. The analysis of the source of flux measurement was within 2 km of the tower with the size of one grid represent 20 × 20 meter.

Average of source weight function (fp(x)) were fluctuated from year to year. Highest fp(x) observed from 2009 (0.75×10^{-2}) followed by 2008 (0.70×10^{-2}) which were also years with less *P*. Low maximum fp(x) observed in year 2003, 2011, and 2012 (0.46×10^{-2}, 0.45×10^{-2}, 0.45×10^{-2} respectively) whereas middle range of maximum fp(x) observed in year 2004, 2006, and 2010 (0.64×10^{-2}, 0.54×10^{-2}, 0.57×10^{-2} respectively). However most of the fp(x) for all years located in the class ≤0.00001.

Table 7. Percent cumulative of fp(x)

No	Fp(x)	% cumulative							
		2003	**2004**	**2006**	**2008**	**2009**	**2010**	**2011**	**2012**
1	**≤0.00001**	71.66	74.11	74.39	76.04	75.79	74.38	74.98	74.23
2	**≤0.0005**	99.70	99.66	99.66	99.63	99.64	99.65	99.64	99.65
3	**≤0.001**	99.89	99.87	99.85	99.84	99.85	99.85	99.85	99.86
4	**≤0.002**	99.97	99.96	99.95	99.94	99.94	99.96	99.94	99.95
5	**≤0.004**	100.00	99.99	99.99	99.99	99.99	99.99	100.00	99.99

6	**≤0.006**	100.00	100.00	100.00	100.00	100.00	100.00	100.00	100.00
7	**≤0.008**	100.00	100.00	100.00	100.00	100.00	100.00	100.00	100.00

Then, how were the footprint spatially distributed? Footprint climatology graphs were drawn for annual footprint to observed the source of the footprint. Most of the time, footprint came from Northeast – Southeast and Southwest – Northwest with 2011 as an exception (i.e. it distributed to all direction around the tower). All the time, strong fp(x) were come from radius less than 100 meter, the medium fp(x) ($\pm$ 0.05×10^{-3}) came from radius 100-200 meter, and the weaker fp(x) observed beyond radius 200 meter.

The representativeness of footprint at HFK was analyzed using satellite images in 2004 and 2011. Ikonos image (acquisition date March 18th 2004) was used for year 2004 and google images (acquisition date July 9th 2011) was used for 2011 and then land cover interpretation using visual interpretation was conducted within 2 km around the tower. Within 200 meter around the tower, the dominant land cover representation was rice-paddy field for both years (i.e. 48.1% in 2004 and 54.5% in 2011). Rice-paddy field also became the major land cover from 200 to 500 meter around the tower (i.e. 81% in 2004 and 66% in 2011).

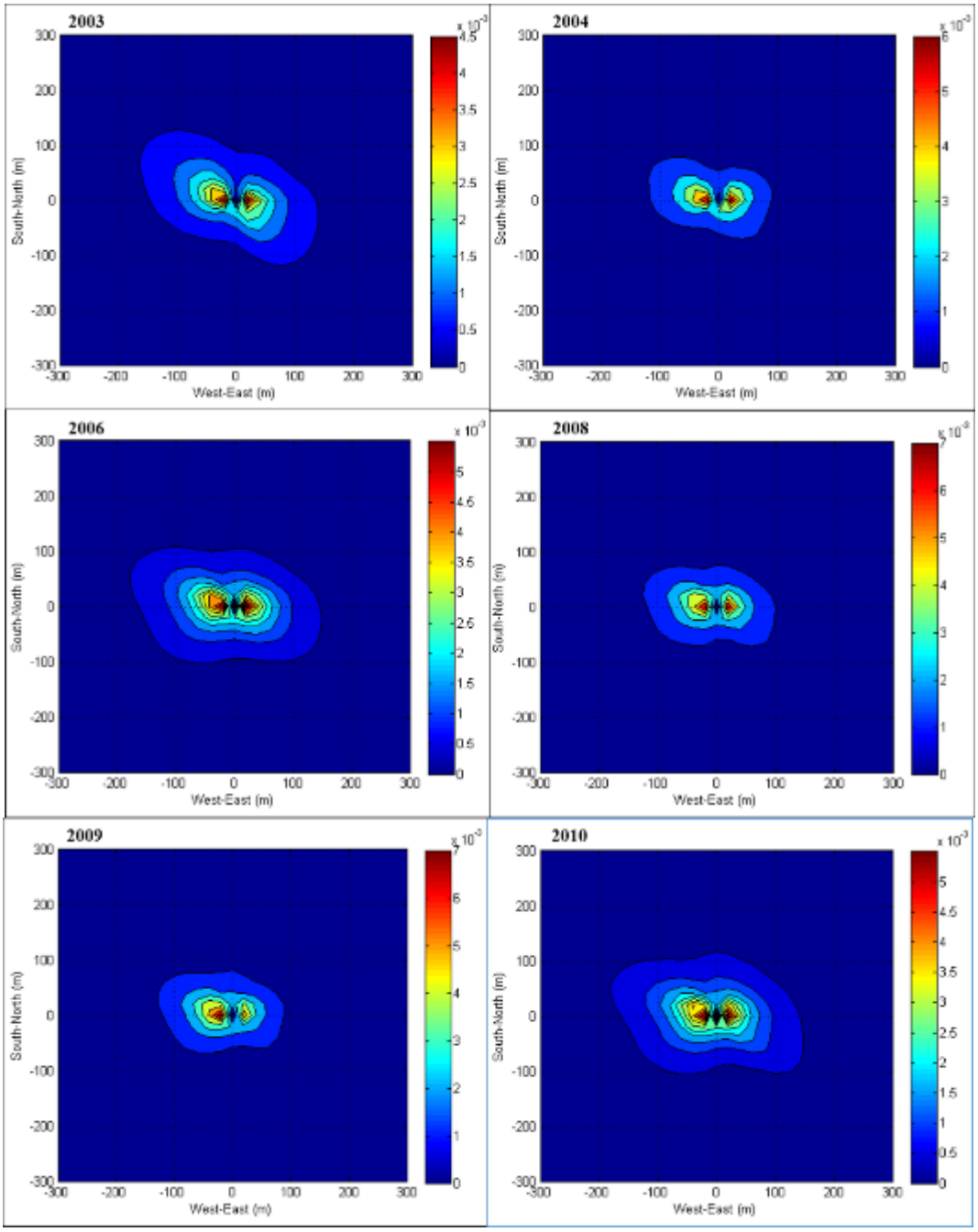
2003
2004
2006
2008
2009
2010
South-North (m)
West-East (m)

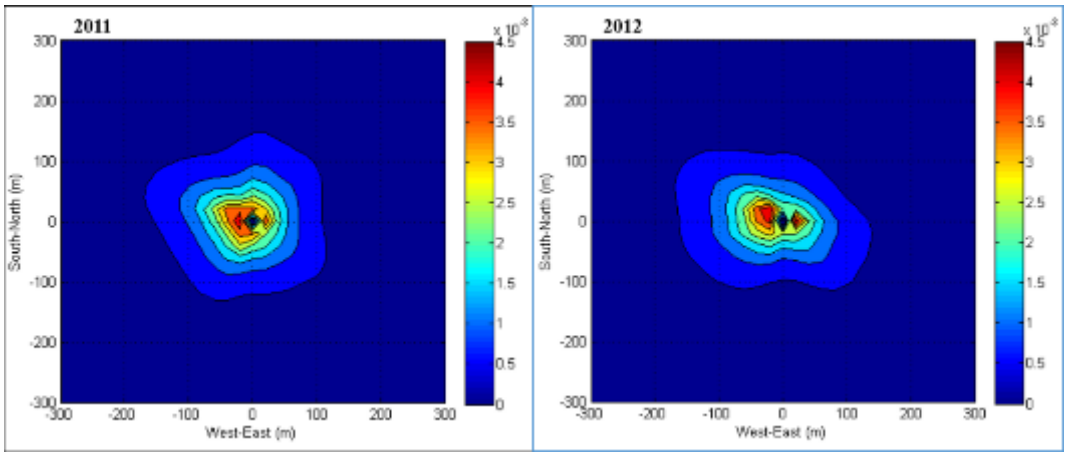

Figure 8 Annual footprint climatology from 2003 to 2012.

Table 8. Land cover representation around the flux tower.

Distance (m)	Land cover representation (%)											
	tall canopy		rice-paddy		other crops		settlement		livestock		others	
	2004	2011	2004	2011	2004	2011	2004	2011	2004	2011	2004	2011
0-200	3	1.9	48.1	54.5	43.9	38.7	2.6	0.6	2.3	4.3	0	0
200-500	0.1	0	81.5	66.0	10.5	18.5	6.4	6.3	0.3	2.4	1.2	6.8
500-1000	11.6	8.9	73.4	61.6	7.1	20.5	2.6	4.1	0.8	0.1	4.5	4.7
1000-2000	42.9	41.2	42.4	26.9	7.8	21.9	4.3	5.4	0.1	0.3	2.6	4.3

3.3 Evapotranspiration Limit

Based on climate meteorological condition with monsoon season happen in the growing season and land cover type which is agricultural farmland where people management is always involved (i.e. irrigation practice), *ET* in HFK site is limited by available energy rather than water supply. Here, the budyko curve was used to show that condition.

Based on Budyko framework, Budyko curve is used to simulate evapotranspiration is a function of an aridity index (*DI*) in a simple supply-demand framework (Arora, 2002). When water is limiting, the maximum possible *ET* is *P* and when energy is limiting, the maximum possible *ET* is ET_p, *ET* approaches one of these two limits as water or energy become increasingly limiting under steady-state condition (Donohue *et al*. 2007). Arid regions are characterized by a dryness index (*DI*) > 1, and *ET* is limited by the supply of water by *P* with Evaporative Index (*EI*) =1, while humid regions have a low value of *DI* <1, and *ET* is limited by radiative energy and thus *EI* < 1 (Kleidon *et al*., 2014) .

Table 9. Annual and seasonal value of ET_p (mm)

Year	2003	2004	2006	2008	2009	2010	2011	2012	Avg	std
winter	48	47	44	48	53	60	53	48	**50**	**5**
spring	179	189	184	202	241	204	241	202	**205**	**23**
summer	244	310	290	318	276	292	276	318	**290**	**24**
fall	164	154	155	163	168	170	168	163	**163**	**6**
Annual	**634**	**700**	**672**	**731**	**738**	**726**	**738**	**731**	**709**	**35**

ET_p calculated to draw Budyko curve at HFK. Annual average of ET_p at HFK was 709 ± 35 mm which accounted for 48 ± 0.09 % of annual *P*. From annual variation, ET_p showed increasing pattern. Seasonally, summer gave big contribution to annual ET_p (41 ± 0.03 %).

The Budyko curve for annual, growing-nongrowing, seasonal, and monthly

time scale was drawn to observe those phenomena. At annual time scale, *DI* values (x-axis) for all years observed to be less than 1 which means that *ET* is limited by the amount of available energy and *ET* is approaching ET_p but still not exceed the demand limit (ET=ET_p) which imply that the source of supply coming from *P*. Based on *DI*, 2003 was the wettest year and 2008 was the driest year which also can be seen from climatological condition were the highest annual *P* occurred in year 2003 and the lowest annual *P* occurred in year 2008. All observation years are within the demand limit and expected value represent by Budyko curve which implied that *ET* for annual time scale in HFK can be represented by available water (*P*) and available energy (ET_p) with the absent of other properties of the landscape.

Decreasing the temporal scale to growing and non-growing season from 8 years resulted in *DI* of all of the observation points are still less than 1. In this case, growing season period shows the observation values are under the demand limit and most of them are close to expected value represent by Budyko curve. In the other hand, in non-growing season, *EI* for most of the observed points are over the limit ($ET = ET_p$) which can imply that supply of water is not only come from *P* and observation values were mostly greater than expected value with large distribution. It may imply that *ET* in growing season still controlled by *P* and ET_p while in the dormant season, other factors also take an effect such as seasonal variation of *P* and ET_p. Some of the observation data in non-growing season were

approaching *DI*=1 line which implied the increase in *ET* is getting closer to the available water from *P*.

In the seasonal temporal scale, each season can be easily distinguised based on its water supply and evaporative demand. As expected, the deviation of observational data with the expected value is getting bigger and some of the observation data were approaching the *DI*=1 which are implied the transition between energy limited evapotranspiration to water limited evaporation.

Spring, summer, and winter time showed always on wet condition (ET_p<1) on the other hand, fall observed both in wet (ET_p <1) and dry (ET_p >1) condition. Due to monsoon in summer season which is resulted in high amount and intensity of precipitation, summer observation data showed lowest *DI* value and ET/ET_p observed close to the limit (ET=ET_p) while other season showed large distribution. For winter season, all observation value are over the evaporative demand limit.

For monthly temporal scale, the observation values are more dispersed than in other time scales. As expected the majority of observation data are observed in *DI* less than 1 (ET_p <1) which means that even in monthly time scale, *ET* is limited by the amount of available energy than by water supply. 2003, 2010 and 2011 were the year which most of the time are in wet condition (ET_p <1). Deviation from the supply line ($ET \leq P$) can be showed in 2006, 2008, and 2009 which *ET* was 1.1 times *P* or greater may indicate that *P* is more strongly underestimated than *ET* or may

indicate other water supply than *P* which is not measured by rain gauges (William *et al*., 2012).

When applying Budyko framework in the small scale area (l<1000 km^2), *ET* may vary substantially under the influence of local conditions (non-climatic character) such as topography and vegetation which affect albedo and surface temperature that determine the availability of energy (Donohue *et al*., 2007). Even though there are many deviations away from the expected value but those deviations are moving closer to the water and energy limit lines. Deviation away from the energy limit and water limit line happen when *P* and ET_p have seasonal cycles that are out phase with each other (Arora, 2002).

Generally for annual, seasonal and even monthly time scale of the Budyko curve at HFK showed the consistency limiting factor of *ET* which is the availability of energy rather than availability of water. In other words, during the observation period at HFK, the availability of energy is a fraction of the amount required to evaporate the entire annual *P* so that not all *P* are converted into *ET*. The implication of this condition is the change in *ET* is determined by the change in available energy (i.e. $R_s\downarrow$) rather than the change of available water (e.g. *P*).

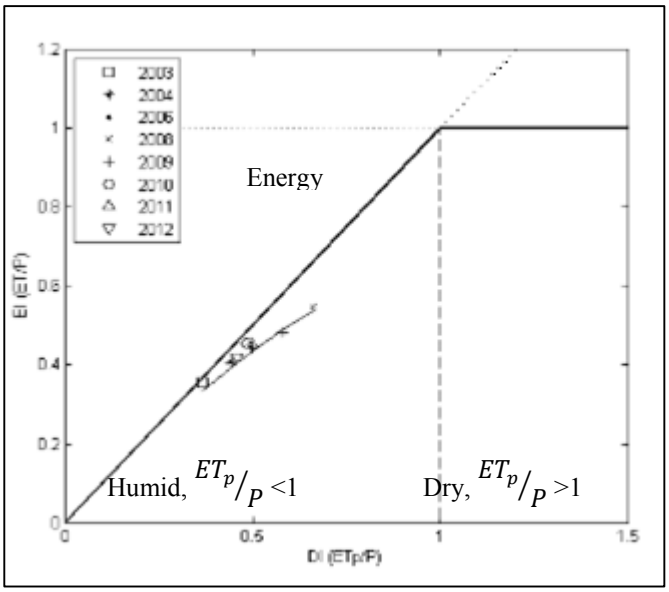

Figure 9 Budyko curve of annual *ET*.

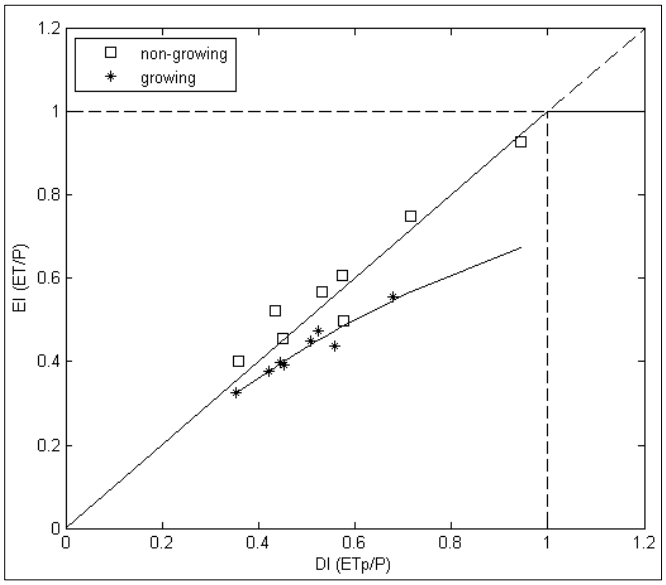

Figure 10 Budyko curve of growing and non-growing season *ET*.

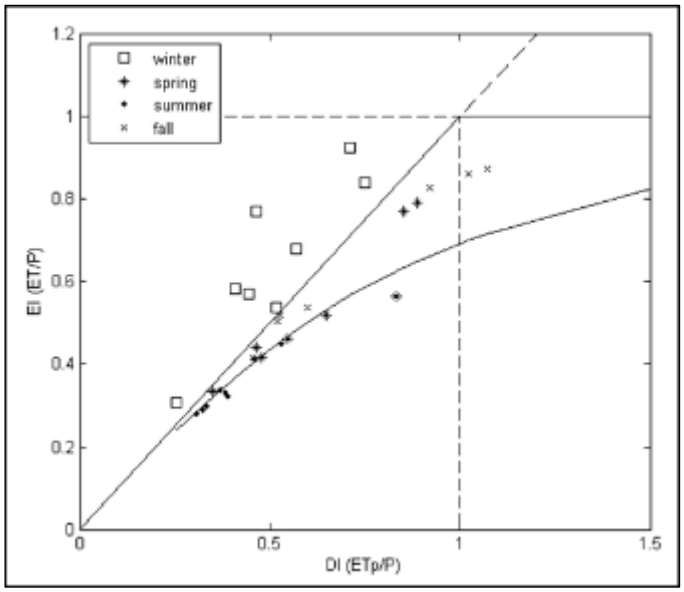

Figure 11 Budyko curve of seasonal *ET* .

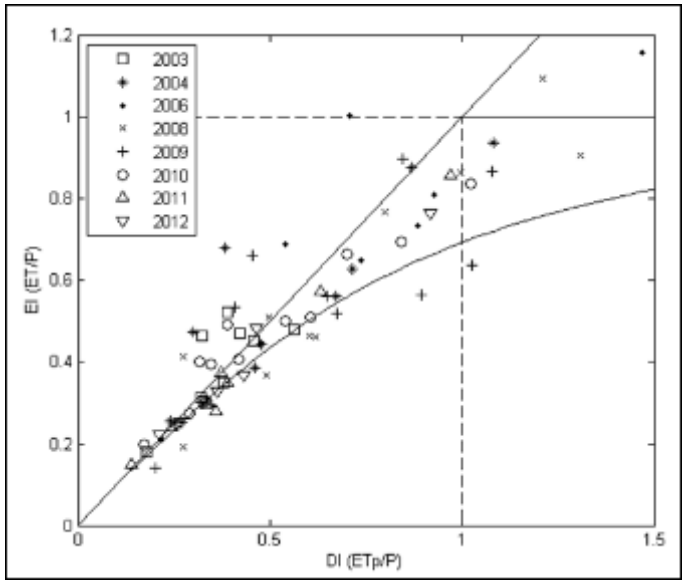

Figure 12 Budyko curve of monthly *ET*.

3.4 Evapotranspiration and Reference Evapotranspiration

The *ET* rate from a reference surface (ET_o) concept introduced to study the evaporative demand of the atmosphere independently of crop type, crop development, and management practices. The only factors affecting ET_o are climatic parameters which express the evaporating power of the atmosphere at a specific location and time of the year and do not consider the crop characteristics and soil factors (Allen *et.al*., 1998). ET_o calculated using globally accepted procedure to estimate ET_o that is the FAO-56 reference crop evapotranspiration equation which is the Penman-Monteith equation for specific reference conditions which based on Shuttleworth and Wallace (2009), humid condition is a prerequisite for its applicability. For the calculation of ET_o, $H+LE$ used to replace R_n-G in energy component to avoid extra energy from soil heat flux measurement and storage term. Sensitivity analysis also conducted for energy, wind, temperature, and vapor pressure component to see the contribution of each component toward ET_o.

Change in energy component value showed the highest contribution to change in ET_o. For 5 % increases in energy component can resulted in increasing ET_o value by 3 %. Other components can only made ET_o value increased by 1 % if there is a 5 % increase in their values. This sensitivity analysis result agreed with the previous analysis of limiting factor of *ET* in HFK (section 3.4).

Table 10. ***ET*o and *ET* (mm y^{-1}) at HFK**

Year	winter		spring		summer		fall		Annual	
	ET_o	*ET*	ET_o	*ET*	ET_o	*ET*	ET_o	*ET*	ET_o	*ET*
2003	117	65	259	172	274	223	222	158	872	618
2004	79	56	201	171	294	277	176	141	750	646
2006	64	55	183	161	255	251	160	130	662	598
2008	77	49	200	162	273	270	147	124	697	604
2009	86	84	217	164	243	231	164	137	710	616
2010	78	73	201	194	261	262	172	153	712	683
2011	70	60	224	215	248	246	168	151	711	672
2012	65	52	201	171	285	290	164	160	714	673
Average	**79**	**62**	**211**	**176**	**267**	**256**	**172**	**144**	**728**	**639**
std	**16**	**11**	**22**	**18**	**17**	**21**	**21**	**12**	**59**	**32**
CV	**20**	**18**	**10**	**10**	**6**	**8**	**12**	**9**	**8**	**5**

Average of annual values of *ET* for 10 years was 639 ± 32 mm y^{-1} and for ET_o was 728 ± 59 mm y^{-1} with coefficient of variation (CV) for annual values of *ET* is 5 and for ET_o is 8. Both annual ET_o and *ET* happen to be lowest in 2006 while the highest ET_o observed in 2003 and the highest *ET* observed in 2010. In the seasonal period, as radiation and temperature increase, ET_o and *ET* value are increasing with peak is observed in summer season for all years. It also observed that most of the time in all season, *ET* doesn't exceed ET_o except in year 2010 and 2012 summer, *ET* value are slightly higher than ET_o value by 1 to 5 mm $season^{-1}$.

How much *P* were converted into *ET* during the observation year were observed for annual and seasonal time scale. Annual average of *P* which was going

back to the atmosphere from *ET* was 44 ± 5 %. In year 2003, with the highest amount of *P*, it observed that only 36 % of annual *P* was converted to *ET*. While in 2012, also with high amount of *P*, 39 % of P was turned into *ET*. In 2008 which had the lowest *P*, 55 % of *P* was converted into *ET*.

ET_o and *ET* value also examined for non-growing (dormant) and growing season. Growing season divided into spring barley growing season and rice-paddy growing season. Growing season divided into spring barley growing season and rice paddy growing season. Based on Kwon *et al*., 2010, spring barley growing season was from April to May and rice paddy growing season was from June to October (planting time on late May to early June and harvest time on late September to early October).

Average both ET_o and *ET* value for 10 years of spring barley growing season expected to be lower than of rice-paddy growing season (158 ± 16 mm and 402 ± 25 mm respectively). For both growing season, ET_o showed the highest value at the beginning of observation years and then fluctuated trough out the years with the variability of 10 for spring barley and 6 for rice-paddy. While *ET* for both crops in the growing season were gradually increasing.

Table 11. ET_o and ET (mm y^{-1}) of spring barley and rice paddy in growing season

Year	Spring barley growing season		Rice-paddy growing season	
	***ET*0**	***ET***	***ET*0**	***ET***
2003	189	128	445	348
2004	149	127	433	392
2006	131	123	378	360
2008	155	133	391	375
2009	167	126	372	345
2010	155	146	396	387
2011	165	162	383	369
2012	156	133	414	421
Average	**158**	**135**	**402**	**375**
std	**16**	**12**	**25**	**24**

Anomaly of ET_o and ET value calculated as the ratio between the difference of the actual value and the mean value with its standard deviation. The highest positive anomaly of ET_o for spring-barley and rice-paddy growing season observed in year 2003 and the highest negative anomaly of ET_o for spring-barley and rice-paddy growing season observed in different years (2006 and 2009, respectively). For ET, the highest positive anomaly observed in 2011 for spring barley growing season and in 2012 for rice paddy growing season which is the opposite with ET_o anomaly which occurred at the beginning of observation years. The highest negative anomaly of ET for spring-barley and rice-paddy growing season observed in 2008 and 2009 respectively which was similar with ET_o that also happen in the middle of observation years.

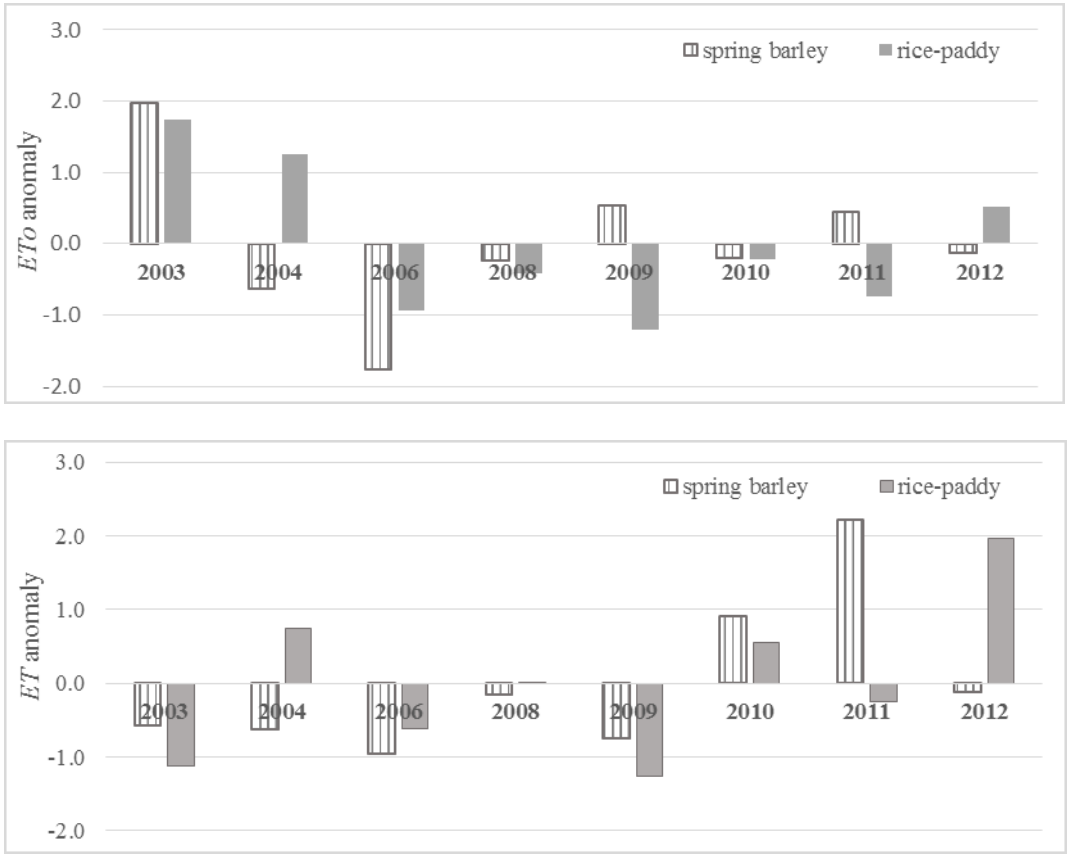

Figure 13 Anomaly of spring barley and rice-paddy *ETo* and *ET* (mm y^{-1}) (baseline 2003-2012).

Based on annual, seasonal, and growing season value of both ET_o and *ET*, *ET* in HFK showed increasing pattern so that similar or even slightly higher than ET_o. Related to the limited controlling factor of *ET* in HFK (i.e. the availability of energy), the increase in *ET* is mostly related to the gradually increasing $R_s\downarrow$ (section 3.1) as the major energy resource for *ET* in HFK.

3.5 Crop coefficient (K_c)

K_c needed for the estimation of crop water requirement which defined as the amount of water required to compensate the evapotranspiration loss from the cropped field and the values for crop *ET* and crop water requirement are identical (Allen *et al*., 1998). K_c value varied due to the characteristics of the crop, transplantation date, grow stage, differences in crop height, crop roughness, albedo, soil, and canopy cover.

K_c value for spring barley growing season and rice paddy growing season (i.e. from April to October), were calculated and documented. Annually average value of K_c for spring barley and rice paddy showed different pattern. Spring barley K_c value showed fluctuation pattern which lowest value in 2003 and then increase until reached first peak in 2006 before decreasing for two following years. The second peak occurred in 2010 before decreasing until the end of observation years. While rice-paddy K_c was increasing g in the beginning of observation years and then stabilized for the rest of the years before was increasing again by the end of observation years in other words, K_c value for rice-paddy showed gradually increasing pattern which also observed in *ET*.

Figure 14 Annual K_c of spring barley and rice-paddy

K_c value commonly observed based on the crop growing stage. K_c value for rice-paddy in different growing stages following FAO rice-paddy growing stage is presented. Other sites rice-paddy K_c values are included for comparison. Single K_c value for non-stressed, well-managed rice-paddy in sub-humid climates recommended by FAO for each growing stage are 1.05 for initial stage, 1.20 for development and middle stage and 0.90-0.60 for late stage. Compare with values from FAO, HFK rice-paddy K_c showed lower value for the initial stage (0.87 ± 0.07), the development stage (1.02 ± 0.08) and the middle stage (1.02 ± 0.08), only the late stage value (0.77 ± 0.10) which is within the range of K_c value recommended by FAO.

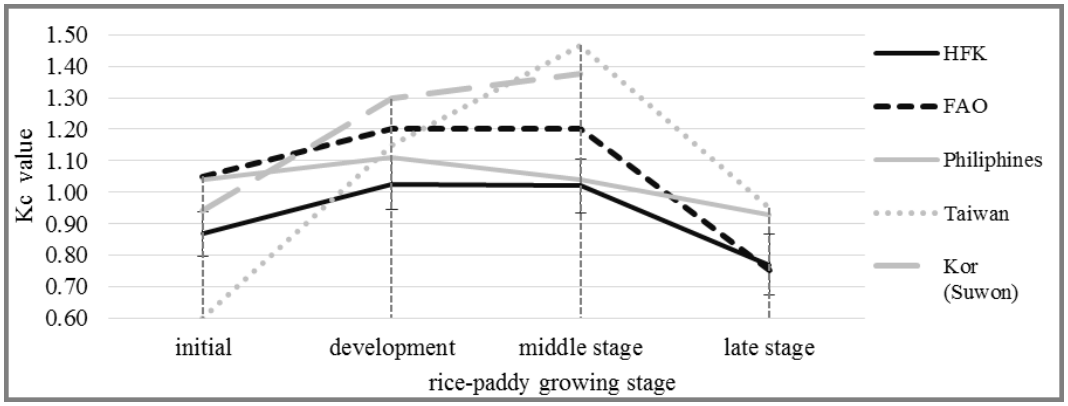

Figure 15 Comparison of rice-paddy Kc value from different sites. FAO (Allen *et al*., 1998), Philiphine (Alberto *et al*., 2011), Taiwan (Kuo *et al*., 2006)

K_c value for rice-paddy in HFK site showed low value compare with other sites. It mostly came from the use of $H+LE$ instead of R_n-G in ET_o calculation. Crop water requirement suggested crop coefficient values for a large number of crops under different climatic conditions which commonly used in places where the local data is not available in FAO-56, however, there is a need for local/regional calibration of K_c under given climatic conditions (Kang *et al*., 2003; Kashyap and Panda 2001). Therefore, the reported values of K_c (e.g. FAO-56) used only in situations when regional data are not available.

The fluctuation pattern of K_c also showed for rice-paddy growing stage. K_c showed increasing pattern for the middle and the late stage and more fluctuated for initial and development stage. The fluctuation of K_c value in HFK is mostly affected by the increase in ET value rather than the decrease in ET_o.

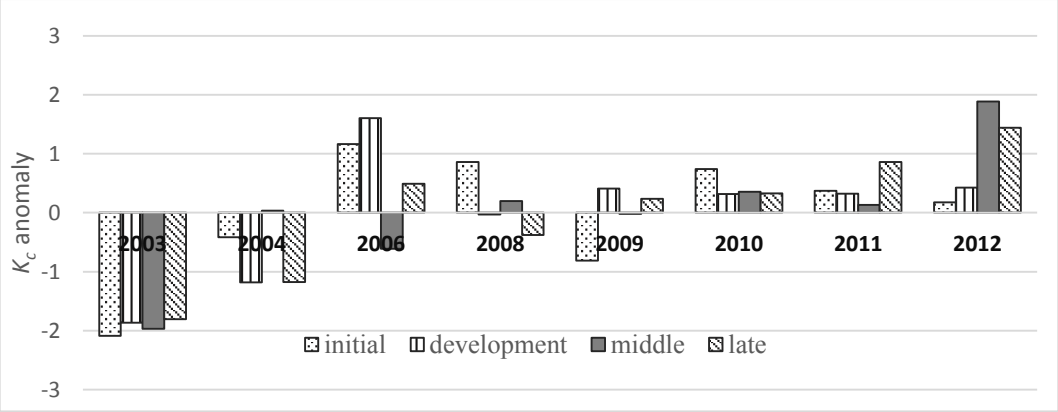

Figure 16 Anomaly of rice-paddy growing stage K_c (baseline 2003-2012).

3.6 Inherent Water Use Efficiency (W_{ei})

Water use efficiency at the ecosystem level is an important ecophysiological index reflecting the coupling relationship between ecosystem water and carbon cycles and the variability of water use efficiency indicated the difference in the coupling between carbon and water cycles (Yu *et al*., 2008). The result of water use efficiency calculation (with and without normalization by *VPD*) from grassland and crop around the globe in recent 20 years documented to see the typical value of each ecosystem (Table 10). It observed that water use efficiency in HFK is happened to be on the low range compare with other sites. It can be due to the difference in the local environmental condition between sites.

Here the year to year and seasonal variation of W_{ei} is analyzed. Average *GPP* for dry days was 568 ± 88 gC m^{-2} yr^{-1} which reduced about half from average

annual *GPP* (1238 ± 94 88 gC m^{-2} yr^{-1}). Year to year variation of *GPP* observed that in 2003 only 45% of total annual *GPP* was used for W_{ei} calculation and 2008 which also observed as a year with least *P,* about 78% of total *GPP* was used for W_{ei} calculation. Other years used about 50 to 60 % of its *GPP.* Seasonally*, GPP* also reduced by half (48 ± 0.5 %). *ET* for a dry days was 307 ± 32 kg H_2O m^{-2} yr^{-1} which account for 52% of total *ET* (639 ± 32 gC m^{-2} yr^{-1}). Year to year variation of *ET* was from 45 to 58% of total *ET*.

The difference in seasonal W_{ei}, *GPP* and *ET* that caused the difference in annual W_{ei} observed for each observation years resulted in two distinctive period. For period 2004-2008, the cause of high annual W_{ei} contributed from high value of W_{ei} in every season (mostly higher than seasonal average W_{ei} value). High seasonal W_{ei} for every season came from different sources. For winter, spring and fall season, both high *GPP* value, and low *ET* values make a contribution for high seasonal W_{ei} value. For summer season, both *GPP* and *ET* are high so that compensate each other. For 2003, 2009-2012, mostly the biggest contributor for annual W_{ei} is only from summer season. In summer season, even though *GPP* is low but *ET* also has low value compare with other seasons (low *GPP* but high *ET*) so that resulted in higher W_{ei} value.

Table 12. Water use efficiency from different sites

No	Lat	Long	Country	ID	Veg	LAI	GPP	*ET*	W	W_{ei}	year	Reference
1	47.12	11.32	Austria	AT-Neu	GRA	6.5			3.8	25.9	1997-2006	Beer *et al*.2009
2	47.29	7.70	China	CH-Oel	GRA	4.9			2.9	17.9	1997-2006	Beer *et al*.2009
3	31.52	122.00	China	CN-Dol	GRA	5.1			2.6	19.2	1997-2006	Beer *et al*.2009
4	50.95	13.51	Denmark	DE-Gri	GRA	4.8			4.4	31.2	1997-2006	Beer *et al*.2009
5	45.64	2.74	France	FR-Lq1	GRA	3.0			2.8	18.8	1997-2006	Beer *et al*.2009
6	45.64	2.74	France	FR-Lq2	GRA	3.0			2.4	16.4	1997-2006	Beer *et al*.2009
7	46.69	19.60	Hungary	HU-Bug	GRA	2.5			2.1	19.5	1997-2006	Beer *et al*.2009
8	41.90	13.61	Italy	IT-Amp	GRA	2.0			3.2	21.5	1997-2006	Beer *et al*.2009
9	46.01	11.05	Italy	IT-Mbo	GRA	2.9			3.0	14.0	1997-2006	Beer *et al*.2009
10	51.97	4.93	Nederland	NL-Ca1	GRA	11.0			2.3	20.6	1997-2006	Beer *et al*.2009
11			Ireland	IE-Dri	GRA				4.8	15.3		Beer *et al*.2007
12	49.43	-112.56	Canada		GRA				1.7			Ponton *et al*.2006
13	37.62	101.33	China	SD	GRA	3.9	424	596	0.7		2003-2005	Hu *et al*. 2008
14	37.67	101.33	China	GCT	GRA	2.8	531	420	1.3		2003-2005	Hu *et al*. 2008
15	30.85	91.08	China	DX	GRA	1.0	199	496	0.4		2004-2005	Hu *et al*. 2008
16	43.55	116.67	China	NM	GRA	1.5	237	284	0.8		2003-2005	Hu *et al*. 2008
17	38.47	8.02	Portugal		GRA				2.5	24.6		Jongen *et al*. 2011
18	44.58	123.50	China	CL	GRA	3.1	592	391	1.5		2007-2010	Xiao *et al*. 2013
19	42.05	116.28	China	DL1	GRA	1.0	323	367	0.9		2006-2007	Xiao *et al*. 2013
20	37.37	101.08	China	HB	GRA	3.8	626	363	1.7		2002-2004	Xiao *et al*. 2013
21	43.55	116.67	China	SZW1	GRA	0.7	62	72	0.9		2010	Xiao *et al*. 2013

22	43.55	116.67	China	SWZ2	GRA	0.6	125	117	1.1		2010	Xiao *et al*. 2013
23	43.55	116.68	China	XLH2	GRA	0.5	484	176	2.8		2006-2007	Xiao *et al*. 2013
24	44.13	116.33	China	XFS	GRA	1.0	136	287	0.5		2004-2006	Xiao *et al*. 2013
25	47.21	8.41	Swiss	Cha	GRA		940	181	4.2		2010-2011	Wolf *et al*. 2013
26	47.29	7.73	Swiss	Oen1	GRA		586	196	2.8		2010-2011	Wolf *et al*. 2013
27	47.12	8.54	Swiss	Fruebuel	GRA		809	233	3.3		2010-2011	Wolf *et al*. 2013
28	50.55	4.74	Belgium	BE-Lon	CRO	5.3			2.8	17.4	1997-2006	Beer *et al*.2009
29	51.10	10.91	Denmark	DE-Geb	CRO	4.0			4.0	27.4	1997-2006	Beer *et al*.2009
30	50.89	13.52	Denmark	DE-Kli	CRO	9.7			3.6	25.0	1997-2006	Beer *et al*.2009
31	47.84	19.73	Hungary	Hu-Mat	CRO	4.0			2.3	17.1	1997-2006	Beer *et al*.2009
32	36.61	-97.49	US	US-ARM	CRO	2.1			1.6	18.8	1997-2006	Beer *et al*.2009
33			Denmark	DK-Ris	CRO				4.3	15.4		Beer *et al*.2007
34	42.05	116.28	China	DL2	CRO	2.4	347	328	1.1		2006-2007	Xiao *et al*. 2013
35	**34.55**	**126.57**	**Korea**	**HFK**	**CRO**		**568**	**307**	**2.0**	**16.4**	**2003-2012**	**This study**

Table 13. Annual and seasonal *GPP, ET, VPD* and W_{ei}

Year		2003	2004	2006	2008	2009	2010	2011	2012	Avg	std
GPP **gC m^{-2} season^{-1}**	winter	49	72	52	87	60	41	48	46	57	15
	spring	110	136	130	151	125	115	99	103	121	16
	summer	191	350	260	303	183	195	215	291	249	58
	fall	106	146	158	141	140	103	191	147	142	26
g C m^{-2} yr^{-1}	**Annual**	**457**	**704**	**601**	**681**	**509**	**454**	**553**	**587**	**568**	**88**
ET **KgH2O m^{-2} season^{-1}**	winter	27	27	24	33	40	36	36	28	31	11
	spring	67	71	66	67	91	82	105	90	80	18
	summer	93	159	116	130	90	102	103	145	117	22
	fall	80	82	73	55	61	67	99	109	78	12
kgH2Om^{-2} yr^{-1}	**Annual**	**267**	**338**	**278**	**286**	**282**	**288**	**344**	**373**	**307**	**32**
VPD **hPa**	winter	4	4.9	3.9	4	4	3.3	3.2	2.8	3.7	0.6
	spring	7.1	8	6.3	7.7	8.9	6	6.4	6.7	7.1	0.9
	summer	6.4	10.4	6.7	8.1	7.6	7.6	7.6	7.3	7.7	1.1
	fall	8.3	10.7	9.1	9.2	9.5	7.8	8	7.3	8.7	1
	Annual	**6.4**	**8.5**	**6.5**	**7.2**	**7.5**	**6.2**	**6.3**	**6**	**6.8**	**0.8**
W_{ei} **gC kgH2O^{-1} hPa ((GPP/*ET*)*VPD)**	winter	9.7	17.1	9.2	12.7	6.5	6.0	5.1	6.5	9.1	3.8
	spring	16.6	18.6	17.7	23.4	14.8	10.9	7.4	9.7	14.9	4.9
	summer	19.5	28.1	25.7	23.7	22.7	20.4	19.2	22.4	22.7	2.9
	fall	13.0	22.3	20.9	27.0	23.9	14.0	17.9	11.1	18.8	5.3
	Annual	**14.7**	**21.5**	**18.4**	**21.7**	**17.0**	**12.8**	**12.4**	**12.4**	**16.4**	**3.6**

Growing season average value of W_{ei} and K_c for barley and rice-paddy growing season also been observed to see the relationship between the change in both variables. Spring barley W_{ei} was increasing from 2003 to 2008 (even though there was a decrease in 2006) and after 2008, W_{ei} tended to decrease. K_c for spring barley showed no pattern related to the change in W_{ei}. W_{ei} for rice paddy was increasing in the beginning and then maintaining in high W_{ei} for 4 years then started to decrease again at the end of observation years while K_c value is gradually increasing.

Table 14. Spring barley and rice-paddy growing season of *GPP, ET, VPD* and W_{ei}

Year		2003	2004	2006	2008	2009	2010	2011	2012	avg	std
Spring barley	***GPP***	84	94	89	119	84	97	71	81	**90**	**13**
	ET	52	50	48	58	70	69	69	75	**61**	**10**
	W_{ei}	18.5	19.6	18.0	21.7	15.4	12.1	8.7	10.4	**15.6**	**4.4**
	K_c	0.68	0.87	0.99	0.89	0.78	0.97	0.93	0.87	**0.87**	**0.1**
Rice-paddy	***GPP***	285	474	400	420	302	278	387	399	**368**	**67**
	ET	159	231	176	178	142	151	192	224	**182**	**31**
	W_{ei}	17.9	26.6	25.3	25.5	24.8	19.4	19.8	18.7	**22.2**	**3.4**
	K_c	0.78	0.89	0.97	0.95	0.94	0.97	0.97	1.04	**0.94**	**0.1**

3.7 Gap Filling in Flux Data and Carbon Balance

3.7.1 Flux Data Gap-Filling

The eddy covariance method delivers continuous data sets of mass and energy exchange between ecosystem and the atmosphere. However, gaps due to unfavorable micro-meteorological conditions and due to instrument failure are inherent in the data stream. Thus, a standardized filling of those gaps is necessary to obtain daily, monthly or annually integrated balances.

Three different gap-filling methods used in this flux data processing that are friction velocity correction (*u**), light response curve (*LRC*) and Van Gorsel (*VG*) method. For annual time scale, the different between three methods in each year were lower compared with year to year different in each method (coefficient of variation (CV) from 6 to 9) with *u** and *VG* method showed high deviation. As shown in Table 2, annual *GPP* value from different gap-fill method show similar result in every year except in 2012 which showed highest difference among gap fill methods (100-200 g C m^{-2} $year^{-1}$), the variability of *GPP* in relation to the mean value are range from 1 to 7 with the highest variability occurred in 2012. For *RE*, the deviation of different gap fill methods was higher than in *GPP* with CV range from 2 to 11 while inter-annual variability showed the highest deviation in *LRC* method.

Table 15. Annual *GPP*, *RE*, and *NEE* for 3 different method (g C m^{-2} y^{-1})

Year		2003	2004	2006	2008	2009	2010	2011	2012	AVG	STD
	u*	1193	1359	1396	1396	1195	1228	1109	1113	**1249**	**112**
	LRC	1213	1307	1318	1350	1147	1254	1160	1216	**1246**	**70**
GPP	**VG**	1192	1316	1353	1352	1219	1204	1082	1033	**1219**	**112**
	AVG	**1200**	**1327**	**1356**	**1366**	**1187**	**1229**	**1117**	**1120**		
	std	**10**	**23**	**32**	**21**	**30**	**21**	**32**	**75**		
	u*	1140	1215	1274	1209	1100	1249	1162	1250	**1200**	**57**
	LRC	1161	1043	1049	1073	907	1227	1157	1388	**1126**	**135**
RE	**VG**	1107	1067	1127	1088	1097	1157	1064	1056	**1095**	**32**
	AVG	**1136**	**1109**	**1150**	**1123**	**1035**	**1211**	**1128**	**1231**		
	std	**22**	**76**	**93**	**61**	**90**	**39**	**45**	**136**		
	u*	-53	-144	-122	-187	-95	22	52	137	**-49**	**103**
	LRC	-52	-264	-269	-277	-240	-28	-3	172	**-120**	**156**
NEE	**VG**	-85	-248	-226	-265	-122	-47	-18	24	**-123**	**104**
	AVG	**-63**	**-219**	**-206**	**-243**	**-152**	**-18**	**10**	**111**		
	std	**15**	**53**	**61**	**40**	**63**	**29**	**30**	**63**		

Due to the small variability of averaging the result of three gap filling method which is less than the interannual variability of each gap-filling method then for analysis, averaging of three gap-filling method was conducted in this research.

3.7.2 Carbon Balance

The net ecosystem exchange (*NEE*) of CO_2, gross primary productivity (*GPP*), and ecosystem respiration (*RE*) were documented based on 10-years flux observation data at HFK. Below, their annual and seasonal magnitudes and variations are presented.

The annual average of *GPP* was 1235 ± 90 g C m^{-2}, which showed an increase from 2003 (1200 g C m^{-2}) to 2008 with a maximum of 1366 g C m^{-2}. In 2009, *GPP* started decreasing and then fluctuated for the remaining years. The summer season was the largest contribution (602 ± 35 g C m^{-2}) to the annual *GPP*. The annual average of *RE* was 1139 ± 54 g C m^{-2}. *RE* remained relatively constant from 2003 to 2008, and then fluctuated with a maximum of 1231 g C m^{-2} in 2012. Again, the summer season contributed the most (493 ± 38 g C m^{-2}) to the annual *RE*.

Except 2003, the *NEE* results indicated that the agricultural ecosystem (defined by the tower flux footprint) at the HFK site gradually changed from moderate carbon sink to weak carbon source in 2010. The summer seasons were always the largest carbon sink, but its magnitude continuously decreased from 2003

to 2012, resulting in HFK to be carbon neutral in 2010 and 2011 and a weak carbon source in 2012.

Table 16. Annual and seasonal *GPP*, *RE*, and *NEE*

Year		2003	2004	2006	2008	2009	2010	2011	2012	Avg	Std
GPP	winter	109	143	105	111	124	82	75	80	104	22
	spring	272	289	315	321	214	254	196	194	257	48
	summer	564	635	647	635	550	620	566	599	602	35
	fall	256	259	289	299	298	273	281	247	275	18
	Annual	**1200**	**1327**	**1356**	**1366**	**1187**	**1229**	**1117**	**1120**	**1238**	**94**
RE	winter	130	121	101	114	109	121	106	134	117	11
	spring	241	247	246	243	206	258	196	241	235	20
	summer	484	465	516	476	431	498	499	572	493	38
	fall	281	275	287	290	289	334	327	284	296	21
	Annual	**1136**	**1109**	**1150**	**1123**	**1035**	**1211**	**1128**	**1231**	**1140**	**57**
NEE	winter	22	-22	-4	3	-15	39	31	54	14	26
	spring	-31	-42	-70	-77	-9	4	0	47	-22	39
	summer	-79	-170	-131	-159	-119	-122	-67	-27	-109	45
	fall	25	15	-2	-9	-9	61	45	37	21	24
	Annual	**-63**	**-219**	**-206**	**-243**	**-152**	**-18**	**10**	**111**	**-97**	**119**

Annual value in g C m^{-2} yr^{-1} and seasonal value in g C m^{-2} $season^{-1}$.

Anomaly from the average value (2003-2012) was observed for *GPP*, *RE*, and *NEE*. Positive anomaly of *GPP* observed happen in the early years (2004-2008), while other year showed negative anomaly which became larger in latest year (2011-2012). *RE* showed small fluctuation from the average value in early until middle observation years (2003-2008) and then the fluctuation became bigger resulted in larger negative deviation in year 2009 and larger positive deviation in

2010 and 2012 while in 2011 was slightly below average value. The anomaly of *NEE* showed reversed pattern compare with *GPP*. From 2004 to 2009, the carbon that was absorbed, were higher than the average especially in year 2008 but it then became weaker in 2009. From 2010 to 2012, the carbon absorption continued to be weaker.

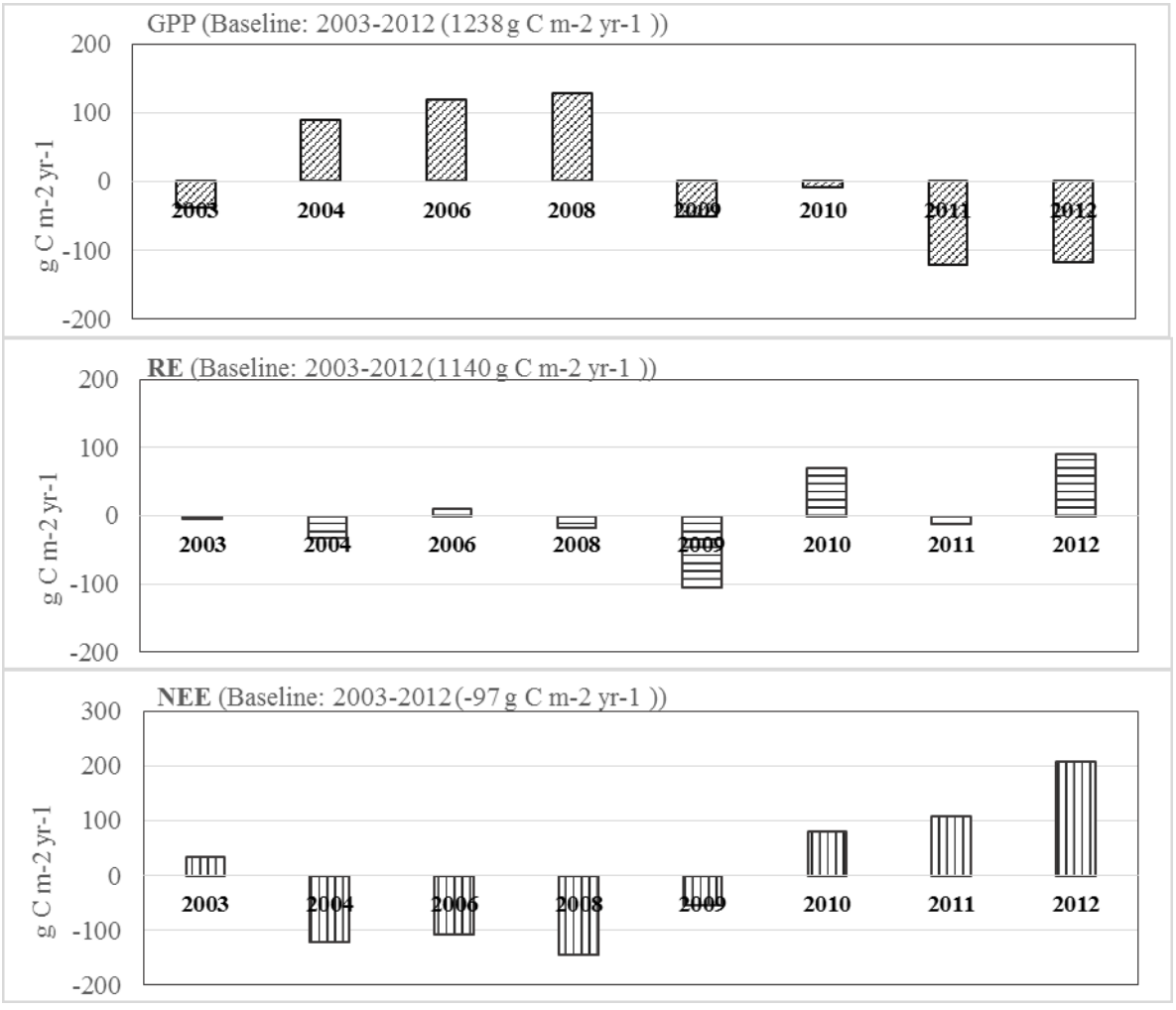

Figure 17 Anomaly of *GPP, RE,* and *NEE* during the observation period.

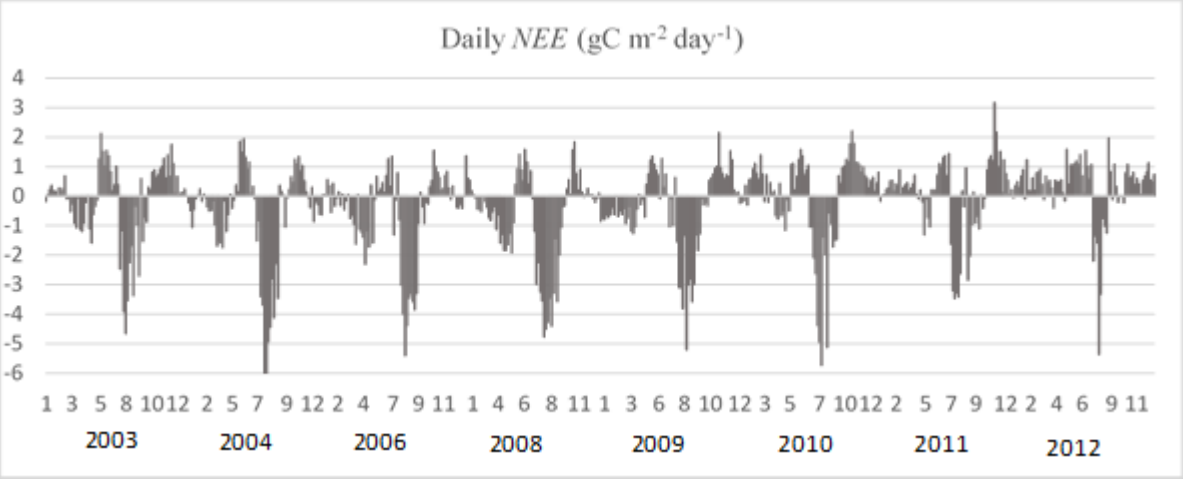

Figure 18 Daily *NEE* during the observation years.

The occurrence of the mid-season depression in *NEE* was reported in Kwon *et al* (2009; 2010) for 2004, 2006 and 2008. At HFK, such periods of the reduced *NEE* (in late-May to mid-July) between the bimodal peaks were clearly observed from 2003 till 2010, and then very much weakened in 2011 and 2012 when bimodal peaks became no longer obvious. The first peak of *NEE* that usually occurred in early-to mid-spring, shifted more toward mid-spring and the second period of carbon absorption after the depression became shorter, causing the ecosystem to be weak carbon source.

3.8 Energy and Entropy Balance

3.8.1 Energy Balance

Study of entropy production (σ) should started with the ecosystem energy balance in which radiation (R_n) is dissipated by *LE* (i.e. evapotranspiration), *H* (i.e. thermal), ecosystem heat flux (*G*), and any net energy flux owing to carbon fixation and the growth, maintenance, and reproductive sources of ecosystem respiration. Here energy balance was assessed through energy balance ratio (*EBR*) without considering *G* and any net energy flux.

Integrated mean of annual R_n was 2567 (±102) MJ m^{-2} which showed fluctuation pattern from year 2003 to 2006 then slightly increasing pattern from 2006 to 2012. Lowest R_n was happened in 2006 (2380 MJ m^{-2}) and the highest R_n was observed in 2012 (2698 MJ m^{-2}). Annually, *H* was ranged from 451 to 688 MJ m^{-2} with the lowest *H* observed in 2003 (451 MJ m^{-2}) and the highest *H* observed in 2011 (688 MJ m^{-2}). *LE* was ranged from 1459 to 1667 MJ m^{-2} with the lowest *LE* was happened in 2006 (1474 MJ m^{-2}) and the highest *LE* was observed in 2010 (1667 MJ m^{-2}). Annually average of β was 0.39 ± 0.05 with lowest β observed in year 2003 (0.30) and highest β observed in 2008 and 2009 (0.45).

Table 17. Annual Bowen ratio

Year	2003	2004	2006	2008	2009	2010	2011	2012	average	std
***H* (MJ m^{-2} y^{-1})**	451	547	603	661	670	592	688	590	**600**	**72.1**
***LE* (MJ m^{-2} y^{-1})**	1507	1576	1459	1474	1503	1667	1640	1643	**1559**	**77.7**

β	**0.30**	**0.35**	**0.41**	**0.45**	**0.45**	**0.36**	**0.42**	**0.36**	**0.39**	**0.05**

Energy balance ratio (*EBR*) was calculated without considering *dG/dt* so that *EBR*= (*H+LE) / R_n*. Linear regression between *H+LE* and R_n and the r square are ranging between 0.80 to 0.93. EBR showed ranged from 0.80 to 0.90 which the highest EBR observed in 2011 and lowest EBR observed in 2003 and 2004.

Table 18. Annual Energy Balance Ratio

Year	R_n (MJ m^{-2})	*H+LE* (MJ m^{-2})	EBR	intercept	slope	r^2
2003	2442	1958	0.80	0.40	0.74	0.91
2004	2645	2123	0.80	0.23	0.77	0.91
2006	2380	2063	0.87	0.80	0.74	0.80
2008	2531	2135	0.84	0.41	0.78	0.93
2009	2642	2174	0.82	0.82	0.71	0.91
2010	2602	2259	0.87	0.69	0.77	0.89
2011	2595	2328	0.90	0.58	0.82	0.89
2012	2698	2233	0.83	0.23	0.80	0.92

3.8.2 Entropy Balance

The entropy budget analysis was used to identify the agricultural system state at HFK by applying thermodynamic approach. This was the first attempt to quantifying the system sustainability of the agricultural ecosystem at HFK. Agricultural ecosystem at HFK as an open system under anthropogenic pressure is an example of any ecosystem that existed in the world today. Whether the system

can survive and maintained its integrity or became vulnerable and then dying can be identified by the ecosystem processes and emerge.

Based on Svirezhev (2008), the increase in σ should be compensated for the transfer of entropy out from the system to either equal or even less to maintain the system life or the current configuration. If accumulation of system entropy by internal production and entropy transfer into the system is not balanced with the transfer of entropy out from the system then the system will be going closer to equilibrium or move to new equilibrium. Assuming that agricultural ecosystem as a natural ecosystem under anthropogenic impact (i.e. agricultural management), the system entropy production is correspond to anthropogenic impact to the ecosystem while entropy transfer remains as a natural ecosystem (Svirezchev, 2005). And then the growth of entropy in the system is usually associated with different processes of degradation so that either the amount of entropy accumulated by the system or the rate of entropy production can be used to measure the degradation of the system (Eulenstein, 2010). In other words, the quantity of the entropy overproduction used as an indicator of the degradation of the ecosystems under anthropogenic pressure (Svirezhev and Svirejeva-Hopkins, 1997).

How about agricultural ecosystem at HFK? In the case of HFK, anthropogenic impact to ecosystem observed by the accumulated entropy in the system which could not be transferred or still remain in the system. The annual

mean of internal entropy production (σ) at HFK integrated during the study period was 12.88 (±0.35) MJ m^{-2} K^{-1} yr^{-1}. Incoming shortwave radiation (σ_{Rs}) contributed on average 97 of the internal entropy production and the rest of σ was coming from incoming longwave radiation (σ_{Rl}). The integrated of annual mean of *J* was showing negative sign (-11.89 ± 0.36 MJ m^{-2} K^{-1} yr^{-1}), indicating a net entropy transfer from the system to the environment however the amount of entropy that exported was smaller compared to σ.

Year to year variation of σ showed that in 2003, the magnitude of σ was lowest compared with other years (12.68 MJ m^{-2} K^{-1} yr^{-1}) then increased in 2004 (13.68 MJ m^{-2} K^{-1} yr^{-1}). From 2004 to 2012, σ were fluctuated with average 13.36 ± 0.24 MJ m^{-2} K^{-1} yr^{-1}. Overall, annual σ showed that during the observation period the amount of entropy that come into the system is almost same even though there were small changed in the beginning and slightly fluctuated. It may indicated that there was no major change in this agricultural ecosystem both naturally and human intervention which could causing the drastically change in σ.

The interannual variation of *J* was smaller than that of σ, and the magnitude was comparable to that of σ. It was decreased in the beginning then maintaining its magnitude for the rest of the year. The major determinant of *J* was the components associated with longwave radiation and latent heat flux, which accounted for about 90 % of annual *J*. The contribution of $J_{Rs\downarrow}$ was smallest.

From year to year, entropy that went out from the system was fluctuated from 87 to 93% due to the fluctuation of both production and transfer. However the change in production and transfer of entropy showed small fluctuation during the observation year.

The changes in σ and J affect the time rate of change in system entropy ($^{dS}/_{dt}$) which also showed fluctuation pattern during the observation period however $^{dS}/_{dt}$ was always positive. It implied that the change in σ is not fully compensated by J out to the ecosystem, there were remaining redundant entropy in the system.

Table 19. Annual entropy balance of agricultural ecosystem at HFK

Year	σ_{Rs}	σ_{Rl}	σ	$J_{Rs\downarrow}$	$J_{Rl\downarrow}$	$J_{Rl\uparrow}$	J_{LE}	J_H	J	$\lvert J/\sigma \rvert$	dS/dt	EBR
2003	12.2	0.49	12.7	0.66	37.1	-42.2	-1.50	-5.09	-11.01	0.87	**1.68**	**0.80**
2004	13.3	0.36	13.7	0.72	36.9	-42.4	-1.81	-5.29	-11.89	0.87	**1.80**	**0.80**
2006	12.8	0.26	13.0	0.69	36.6	-42.3	-2.00	-4.89	-11.97	0.92	**1.08**	**0.87**
2008	12.9	0.35	13.3	0.70	37.1	-42.6	-2.20	-4.92	-11.92	0.90	**1.36**	**0.84**
2009	13.2	0.35	13.6	0.72	36.9	-42.4	-2.23	-5.05	-12.01	0.88	**1.58**	**0.82**
2010	12.6	0.49	13.1	0.68	37.2	-42.2	-1.98	-5.62	-11.94	0.91	**1.13**	**0.87**
2011	12.9	0.41	13.3	0.70	36.8	-42.0	-2.31	-5.51	-12.38	0.93	**0.91**	**0.90**
2012	13.2	0.42	13.6	0.71	36.9	-42.2	-1.97	-5.51	-11.99	0.88	**1.60**	**0.83**
Avg	**12.9**	**0.4**	**13.3**	**0.7**	**36.9**	**-42.3**	**-2.0**	**-5.2**	**-11.9**	**0.90**	**1.39**	**0.84**
Std	**0.35**	**0.07**	**0.32**	**0.02**	**0.18**	**0.15**	**0.24**	**0.27**	**0.36**	**0.02**	**0.30**	**0.03**

Unit = MJ $m^{-2}K^{-1}$ $year^{-1}$

Seasonal and growing season contribution to annual entropy budget was analyzed for integrated observation years.

Table 20. Seasonal average of entropy balance of agricultural ecosystem at HFK

Season	σ		J		dS/dt	
	Avg	**Std**	**Avg**	**Std**	**Avg**	**Std**
Winter	0.70	0.10	-0.71	0.08	-0.01	0.06
Spring	1.34	0.17	-1.20	0.14	0.14	0.09
Summer	1.35	0.15	-1.13	0.13	0.22	0.06
Fall	1.03	0.22	-0.92	0.16	0.11	0.07

Unit = MJ $m^{-2}K^{-1}$ $season^{-1}$

3.9 Entropy and the Interconnection with Other Assessment

Assuming that agricultural ecosystem as a natural ecosystem under anthropogenic impact (i.e. agricultural management), the system entropy production is correspond to anthropogenic impact to the ecosystem while entropy transfer remains as a natural ecosystem (Svirezchev, 2005). And then the quantity of the entropy overproduction could be used as an indicator of the degradation of the ecosystems under anthropogenic pressure (Svirezhev and Svirejeva-Hopkins, 1998).

In the case of agricultural ecosystem at HFK, we can see the anthropogenic impact on ecosystem through the increase in internal entropy production of the system while the transfer of entropy was fluctuated. This resulted in the increasing pattern of the time rate of change in system entropy during observation years.

Table 21. Annual entropy budget and other measurement comparison

Annual	σ	J	dS/dt	*NEE*	*GPP*	K_c	*ET*	W_{ei}
2003	12.7	-11.01	1.68	-63	1200	0.69	617	14.7
2004	13.7	-11.89	1.80	-219	1327	0.83	645	21.5
2006	13.0	-11.97	1.08	-206	1356	0.94	597	18.4
2008	13.3	-11.92	1.36	-243	1366	0.83	603	21.7
2009	13.6	-12.01	1.58	-152	1187	0.91	615	17
2010	13.1	-11.94	1.13	-18	1229	0.98	682	12.8
2011	13.3	-12.38	0.91	10	1116	0.95	671	12.4
2012	13.6	-11.99	1.60	111	1120	0.94	672	12.4
Avg	**13.3**	**-11.9**	**1.39**	**-97**	**1238**	**0.88**	**638**	**16.4**
std	**0.32**	**0.36**	**0.30**	**119**	**94.3**	**0.1**	**31.7**	**3.6**

Unit: σ, J, dS/dt = MJ $m^{-2}K^{-1}year^{-1}$, NEE and GPP = gC m^{-2} $year^{-1}$, ET= mm y^{-1}, W_{ei}= gC kg $H2O^{-1}$ hPa.

The agricultural ecosystems at HFK pumped 87 to 93 % of the entropy produced within the system and generally the entropy production and transfer were fluctuated but the production was always higher than transfer. In this case, the small fluctuation of the change in entropy rate showed that the system underwent no drastic changing in term of entropy balance which indicate the system was in the same state during the observation years.

In general, other components show fluctuation pattern with the change in entropy. Annual K_c and *ET* value showed increasing pattern while W_{ei} observed to decrease during the observation period. Seasonal and growing season averages for whole years were observed to see the general contribution of each season. For all

measurements conducted here, spring and summer had the biggest contribution to annual values. Growing season which composed of spring-summer-fall was obviously had biggest contribution to annual values.

Table 22. Seasonal average of daily entropy budget and other measurement

season	σ		J		dS/dt		GPP		K_c		ET		W_{ei}	
	avg	std	avg	std	avg	std	avg	std	avg	std	avg	std	avg	std
winter	0.70	0.10	-0.71	0.08	-0.01	0.06	1.1	0.3	0.86	0.2	0.7	0.2	8.7	4.8
spring	1.34	0.17	-1.20	0.14	0.14	0.09	2.8	0.8	0.86	0.1	1.9	0.5	13.2	4.7
summer	1.35	0.15	-1.13	0.13	0.22	0.06	6.5	2.6	0.98	0.1	2.8	0.5	21.9	8.8
fall	1.03	0.22	-0.92	0.16	0.11	0.07	3.0	1.9	0.84	0.1	1.6	0.7	18.1	7.5

Unit: σ, J, dS/dt = MJ $m^{-2}K^{-1}year^{-1}$, GPP = gC m^{-2} $year^{-1}$, ET= mm y^{-1}, W_{ei}= gC kgH2O^{-1} hPa.

Table 23. Growing and non-growing season average of daily entropy budget and other measurement

season	σ		J		dS/dt		GPP		K_c		ET		W_{ei}	
	avg	std	avg	std	avg	std	avg	std	avg	std	avg	std	avg	std
non-growing	0.86	0.23	-0.83	0.18	0.03	0.08	1.2	0.3	0.83	0.2	0.7	0.2	9.4	4.9
growing	0.20	0.15	1.35	0.14	0.20	0.07	4.5	2.5	0.91	0.1	2.2	0.6	18.5	8.0

Unit: σ, J, dS/dt = MJ $m^{-2}K^{-1}year^{-1}$, GPP = gC m^{-2} $year^{-1}$, ET= mm y^{-1}, W_{ei}= gC kgH2O^{-1} hPa.

4. Conclusions and Future Work

4.1 Summary and Conclusions

Long term eddy covariance (EC) measurements in a typical agricultural ecosystem have been conducted since 2002, resulting in the first 10-year database (from 2003 to 2012) at one of the KoFlux sites, i.e., HFK (Haenam Farmland in Korea). Many studies based on relatively short-term HFK data have produced several publications which addressed topics such as validation of ecological and hydrological models and remote sensing algorithms, the scale of heterogeneity, and ecosystem exchange of carbon, water and energy.

It is worth nothing that the utilization of a decade-long EC dataset may bring out new insights and questions for better understanding of this complex agricultural system with intensive human management. The main purpose of this research was to assess the sustainability of agricultural ecosystem in HFK with the specific objectives: (1) to document the decadal climatology, water use, and energy/carbon balance and (2) to assess the state of this agricultural ecosystem based on thermodynamic perspective. The highlights of the current findings are:

(1) Annually, the average of *P* was 1454 ± 188 mm which was 100 mm higher than 30 years normal. *P* showed decreasing and then increasing pattern with the maximum in 2003 (followed by 2012) and the minimum in 2008 (followed by 2009). Seasonally, largest amount of *P* occurred in summer season up to about

53 ± 5% of the annual total. The *SWC* from May to September for each year ranged from 0.24 to 0.35%.

The annual $R_{s\downarrow}$ was averaged to be 5025 ± 154 MJ m^{-2}. The lowest $R_{s\downarrow}$ of 4724 MJ m^{-2} was observed in 2003 due to the largest amount of *P* in that year. The maximum was observed in 2004 but the amount of P was not necessarily low, indicating that not only an amount but also frequency, intensity and number of rainy days influence the quantity and the quality of radiation. The interannual variation of $R_{s\downarrow}$ generally showed a gradually increasing pattern throughout the study period. The fluctuation of $R_{s\downarrow}$ (which is the main energy source of *ET*) was a major limiting factor of *ET* since the water availability was not limited.

The mean annual T_a was 13.6 ± 0.1 ˚C with a maximum of 14 ˚C in 2004 and the minimum of 13.2 ˚C in 2011. Compared with the normal, it was higher by 0.2 ˚C. T_a showed a gradually increasing pattern.

(2) The footprint climatology for a 2 km grid around the flux tower showed that most of the time the flux footprint came from northwest and northeast. The strongest sources of footprint were within the radius ± 200 meter around the tower for the prevailing wind directions, which were occupied mostly by rice-paddy or barley crop.

(3) The Budyko curve analysis indicated that the *ET* at HFK was limited by available energy rather than water supply for seasonal to annual time scale (i.e.

DI <1). The mean annual *ET* was 639 ± 32 mm, accounting for 44 ± 5 % of the mean annual *P* whereas the mean annual ET_o was 728 ± 59 mm. However, *ET* sometimes exceeded ET_o (e.g., during the summer of 2010 and 2012). The mean total *ET* during the growing seasons of spring barley was 135 ± 12 mm whereas rice-paddy was 375 ± 24 mm. The mean total ET_o during the spring barley growing season was 158 ± 16 mm and 402 ± 25 mm for the rice growing season. ET_o showed a decreasing pattern while the observed *ET* fluctuated with an increasing tendency.

(4) The annual value of K_c was on average 0.88 ± 0.1. During the growing season, the averaged K_c value was 0.87 ± 0.10 for spring barley and 0.94 ± 0.10 for rice. K_c showed fluctuating patterns for the whole period (2003-2012) with an exception for rice crop. There was a sudden increase in 2012 to 1.04 after being stabilized from 2006 to 2011, which was partly due to the decreased ET_o. The local K_c values were lower in comparison with the recommended values from FAO (except for end stage), indicating the important of identification of local K_c values for water management.

(5) The mean annual W_{ei} was 16.4 ± 3.6 gC kg H_2O^{-1} hPa. The interannual variation of W_{ei} was large with higher efficiency during the period from 2004 to 2008. Seasonally, W_{ei} showed highest efficiency in summer (22.7 ± 2.9 gC kg H_2O^{-1} hPa). For the spring barley growing season, W_{ei} was 15.6 ± 4.4 gC kg H_2O^{-1}

hPa whereas the rice W_{ei} was 22.2 ± 3.4 gC kg H_2O^{-1} hPa. In comparison with other agricultural sites, The W_{ei} at HFK is in the lower range likely due to the differences in local environmental conditions. W_{ei} showed a gradually decreasing pattern which was mostly related to the fluctuations in *GPP*.

(6) The mean annual values of *GPP*, *RE* and *NEE* at HFK were 1235 ± 90, 1139 ± 54, and -97 ± 119 gC m^{-2}, respectively. Annually, *GPP* showed a decreasing pattern. Seasonal contribution to the annual *GPP* showed that the summer season (602 ± 35 gC m^{-2}) was the largest contributor. The *RE* stabilized from 2003 to 2008 and then fluctuated for the remaining years. Again, the summer season was the main contributor (493 ± 38 gC m^{-2}). The annual *NEE* showed that the HFK site became a weak carbon source in 2003 (-63 gC m^{-2}), then from 2004 to 2008 became a moderate carbon sink (around -200 gC m^{-2}). In 2009, carbon sink strength was weakened to -152 gC m^{-2} before the site abruptly turned into a carbon source in 2010. The first peak of *NEE*, usually occurred in early- to mid-spring, shifted more toward mid-spring while the second peak of carbon sequestration after the mid-season depression became shorter, causing the ecosystem to be a weak carbon source.

(7) The mean annual R_n was 2567 ±102 MJ m^{-2}, which showed a gradually increasing pattern from 2006 to 2012. The annual *H* ranged from 451 to 688 MJ m^{-2} with the minimum in 2003 and the maximum in 2011. The annual *LE*

ranged from 1459 to 1667 MJ m^{-2} with the minimum in 2006 and the maximum in 2010. The mean annual β was 0.39 ± 0.05 with lowest β observed in 2003 and highest β in 2008 and 2009. *EBR* showed a typical energy budget closure which ranged from 0.80 to 0.90.

The entropy budget at HFK showed that the mean annual σ was 13.36 ± 0.24 MJ m^{-2} K^{-1} while the mean annual *J* was -11.89 ± 0.36 MJ m^{-2} K^{-1}, indicating the net accumulation of internal entropy within the system. The $^{dS}/_{dt}$ fluctuated due to changes in both σ and *J* but remained relatively consistent. Overall, the HFK site annually pumped 88 to 93 % of the entropy produced within the system out to the environment, resulting in an accumulation of entropy within the system.

Based on those actual conditions that were observed at HFK related with system water use which were observed from several components of the system, the conclusions for this research are:

1. The availability of water throughout the year by precipitation and/or groundwater use and irrigation at HFK resulted in *ET* that is energy-limited. *ET* appeared to have been increased, affecting other components of water use (such as K_c and W_{ei}) to change.
2. The variation of K_c was mostly related to the fluctuation of *ET* and the local values of K_c at HFK were lower than those recommended by FAO for rice-

paddies.

3. The observed variations of W_{ei} were mainly associated with changes in *GPP*. The decreasing pattern of *GPP* with the increasing pattern of *ET* resulted in lowering of water use efficiency of the system. The water use at HFK has become inefficient because the system has been losing more water into the atmosphere while the system productivity has been reduced.
4. Inefficient use of water indicated by low W_{ei} and its decreasing trend at FK may be associated with the accumulating entropy within the agricultural ecosystem at HFK for the last decade, which indicates a degradation of the system. However, the excess of entropy within the system due to human intervention with an input of additional energy is the condition that may be avoided if the self-organizing capacity of an ecosystem can be preserved.

4.2 Future Work

This current finding and conclusion are encouraged to further expand and deepen the analysis toward seeking of better options for agricultural management. Several works should be pursued in order to go to further steps, which 1) Compare water use efficiency with actual productivity. 2) Calculating entropy overproduction using different variable (actual productivity, human management practice), 3) analyzing land surface representation effect in every measured and quantified variables, and 4) Analyzing the use of the ground water for agricultural practice. The involvement of social discipline for the future works is recommended.

There are many uncertainties in measuring the sustainability of the system using thermodynamic approach however, from complex system perspective this approach can give better understanding to know how the system is working.

References

Alberto MCR, R Wassmann, T Hirano, A Miyata, R Hatano, A Kumar, A Padre, M Amante. 2011. "Comparison of energy balance and evapotranspiration between flooded and aerobic rice fields in the Philippines". *Agricultural Water Management,* 98: 1417-1430.

Allen RG, Pereira LS, Raes D, Smith M. 1998. "Crop Evapotranspiration: Guidelines for Computing Crop Requirements, Irrigation and Drainage Paper No. 56". Food and Agriculture Organization of the United Nations, Rome, Italy.

AsiaFlux. 2011. HFK: KoFlux Haenam site. Available from: <http://asiaflux.net/index.php?page_id=60> [10 July 2014].

Arora VK. 2002. "The use of the aridity index to assess climate change effect on annual runoff". *Journal of Hydrology*, 265: 164-177.

Baldocchi DD, SB Verma, NJ Rosenberg.1985. "Water use efficiency in a soybean field: influence of plant water stress". *Agricultural and Forest Meteorology*, 34: 53-65.

Beer C, P Ciais, M. Reichstein, D Baldocchi, BE Law, D Papale, JF Soussana, C Ammann, N Buchmann, D Frank, D Gianelle, IA Janssens, A Knohl, B Kostner, E Moors, O Roupsard, H Verbeeck, T Vesala, CA Williams, and G. Wohlfart. 2009. "Temporal and among site variability of inherent water use efficiency at the ecosystem level". *Global Biogeochemical cycles,* 23: GB2018.

Brummer C, TA Black, RS Jassal, NJ Grant, DL Spittlehouse, B Chen, Z Nesic, BD Amiro, MA Arain, AG Barr, CPA Bourque, C Coursolle, AL Dunn, LB Flanagan, ER Humphreys, PM Lafleur, HA Margolis, JH McCaughey, SC Wofsy. 2012. "How climate and vegetation type influence evapotranspiration and water use efficiency in Canadian forest, peatland and grassland ecosystem". *Agricultural and Forest Meteorology*, 153: 14-30.

Budyko MI. 1974. "Climate and Life Vol 18 of International geophysics series". New York, Academic Press.

Campbell GS, JM Norman. 1998. "An Introduction to environmental biophysics, 2nd edition". Springer, New York.

Choi M, SO Lee, H Kwon. 2010. "Understanding of the common land model

performance for water and energy fluxes in a farmland during the growing season in Korea". *Hidrological processes,* 24: 1063-1071.

Donohue RJ, ML Roderick, and TR McVicar. 2007. "On the Importance of including vegetation dynamics in Budyko's hydrological model". *Hydrology and Earth System Sciences,* 11: 983-995.

Eulenstein F, W Haberstock, W Steinborn, YU Svirezhev, J Olejnik, SL Schilindwein, and V Pomaz. 2003. "Prespectives from energetic-theromdynamic analysis of land use systems". *Archives of Agronomy and Soil Science,* 49: 663-676.

Farquhar GD and RA Richards. 1984. "Isotropic composition of plant carbon correlates with water-use efficiency of wheat genotypes". *Australian jurnal of plant physiology,* 11: 539-52.

Foley JA, N Ramankutty, KA Brauman, ES Cassidy, JS Gerber, M Johnston, ND Mueller, C O'Connell, DK Ray, PC West, C Balzer, EM Bennett, SR Carpenter, J Hill, C Monfreda, S Polasky, J Rockstrom, J Sheehan, S Siebert, D Tilman, DPM Zaks. 2011. "Solutions for a cultivated planet". *Nature,* 478: 337-342.

Hsieh CI, Gabriel Katul, Tze-wen Chi. 2000. "Approximate analytical model for footprint estimation of scalar fluxes in thermally stratified atmospheric flows". *Advances in water resources,* 23: 765-772.

Holdaway RJ, AD Sparrow, and DA Coomes. 2010. "Trends in entropy production during ecosystem development in the Amazon Basin". *Philosophical Transactions: The Royal Society B,* 365: 1437-1447.

Hu Z, G Yu, Y Fu, X Sun, Y Li, P Shi, Y Wang, Z Zheng. 2008. "Effect of vegetation control on ecosystem water use efficiency within and among four grassland ecosystems in China". *Global Change Biology,* 14: 1609-1619.

Humes KS, WP Kustas, MS Moran, WD Nichols, MA Weltz. 1994. "Variability of emissivity and surface temperature over a sparsely vegetated surface". *Water resources research*, 30(5): 1299-1310.

Jones JA, IF, Creed, KL Hatcher, RJ Warren, MB Adams, MH Benson, E Boose, WA Brown, JL Campbell, A Covich, DW Clow, CN Dahm, K Elder, CR Ford, NB Grimm, DL Henshaw, KL Larson, ES Miles, KM Miles, SD Sebestyen, AT Spargo, AB Stone, JM Vose, and MW Williams. 2012. "Ecosystem processes and human influences regulate streamflow response

to climate change at long-term ecological research sites". *BioScience,* 624: 390-404.

Jones MM and HM Rawson. 1979. Influence of rate of development of leaf water deficits upon photosynthesis, leaf conductance, water use efficiency, and osmotic potential in sorghum. *Physiologia Plantarum*, 45:103-111.

Jorgensen SE and YM Svirezhev. 2004. "Toward a thermodynamic theory for ecological system". Amsterdam, Elsevier.

Kang M, S Park, H Kwon, HT Choi, YJ Choi, J Kim. 2009. "Evapotranspiration from a deciduous forest in a complex terrain and a heterogeneous farmland under monsoon climate". *Asia-Pasific Journal of Atmospheric Sciences,* 45, 2: 175-191.

Kang M, H Kwon, JH Cheon, J Kim. 2012. On estimating wet canopy evaporation from deciduous and coniferous forest in the Asian monsoon climate. *Journal of hydrometeorology*, 13:950-965.

Kasyap PS and Panda RK. 2001. "Evaluation of evapotranspiration methods and development of crop-coefficients for potato crop in a sub-humid region". *Agricultural Water Management,* 50: 9-25.

Kay JJ and M Boyle. 2008. "Self-Organizing, Holarchic Open Systems (SOHOs). In Walter-Toews D, JJ Kay, NME Lister. ed. "The ecosystem approach: complexity, uncertainty, and managing for sustainability". New York: Columbia University Press.

Keenan TF, DY Hollinger, G Bohrer, D Dragoni, JW Munger, HP Schmid, AD Richardson. 2013. "Increase in forest water-use efficiency as atmospheric carbon dioxide concentrations rise". *Nature,* 499: 324-327 (2008).

Kim J, Q Guo, DD Baldocchi, MY Leclerc, L Xu, HP Schmid. "Upscaling fluxes from tower to landscape: overlaying flux footprints on high-resolution (IKONOS) images of vegetation cover". *Agricultural and Forest Meteorology*, 136: 132-146.

Kleidon A. 2012. "How does the earth system generate and maintain thermodynamic disequilibrium and what does it imply for the future of the planet?". *Philosophical Transactions of the Royal Society A*, 370: 1012-1040.

Kleidon A. 2010. "Life, hierarchy, and the thermodynamic machine of planet Earth". *Physics of Life Reviews*, 7: 424-460.

Kleidon A, M. Renner, and P Porada. 2014. “Estimates of the climatological land surface energy and water balance derived from maximum convective power”. *Hydrology and Earth System Science,* 18: 2201-2218.

Kuglitsch FG, M Reichstein, C Beer, A Carrara, R Ceulemans, A Granier, IA Janssens, B Koestner, A Lindroth, D Loustau, G Matteucci, L Montagnani, EJ Moors, D Papale, K Pilegaard, S Rambal, C Rebmann, ED Schulze, G Seufelt, H Verbeeck, T Vesala, M Aubinet, C Bernhofer, T Foken, T Grunwald, B Heinesch, W Kutsch, T Laurila, B Longdoz, F Miglietta, MJ Sanz, and R Valentini. 2008. “Characterisation of ecosystem water-use efficiency of European forests from eddy covariance measurement”. *Biogeosciences Discuss,* 5: 4481-4519.

Kuo SF, SS Ho, CW Liu. 2006. “Estimation irrigation water requirements with derived crop coefficients for upland and paddy crops in ChiaNan Irrigation Association, Taiwan”. *Agricultural Water Management*, 82: 433-451.

Kwon HH, AF Khalil, T Siegfried. 2008. “Analysis of extreme summer rainfall using climate teleconnections and typhoon characteristics in South Korea”. *Journal of the American Water Resource Association,* 44(2): 4436-448.

Kwon H, TY Park, J Hong, JH Lim, J Kim. 2009. “Seasonality of Net Ecosystem Carbon Exchange in Two Major Plant Functional Types in Korea”. *Asia-Pacific Journal of Atmospheric Sciences*, 45: 149-163.

Kwon H, J Kim, J Hong, JH Lim. 2010. “Influence of the Asian moonson on net ecosystem carbon exchange in two major ecosystem in Korea”. *Biogeosciences*, 7: 1493-1504.

Kwon H, M Choi. 2011. “Error assessment of climate variables for FAO-56 reference evapotranspiration”. *Meteorology Atmospheric Physics,* 112: 81-90.

Kyoung M, J Kwak, D Kim, H Kim, VP Singh. 2011. “Drought analysis based on SPI and SAD curve for the Korean peninsula considering climate change”. In J Blanco and H Kheradmand.ed. “Climate change – geophysical foundations and ecological effects”. InTech.

Law BE, E Falge, L Gu, D Baldocchi, P Bakwin, P Berbigier, K Davis, AJ Dolman, M Falk, JD Fuentes, A Goldstein, A Granier, A Grelle, D Hollinger, IA Janssens, P. Jarvis, NO Jensen, G Katul, K Mahli, G Matteucci, T Meyers, R Monson, W Munger, W Oechel, R Olson, K Pilegaard, KT Paw U, H Thorgeirsson, R Valentini, S Verma, T Vesala, K Wilson, and S Wofsy.

2002. “Environmental controls over carbon dioxide and water vapor exchange of terrestrial vegetation”. *Agricultural and Forest Meteorology*, 113: 97-120.

Lee HC, J Hong, CH Cho, BC Choi, SN Oh, and J Kim. 2003. “Surface exchange of energy and carbon dioxide between the atmosphere and a farmland in Haenam, Korea”. *Korean Jurnal of Agricultural and Forest Meteorology*, 5(2): 61-69.

Lee SJ, J Lee, SJ Greybush, M Kang, and J Kim. 2013. “Spatial and temporal variation in PBL height over the Korean peninsula in the KMA operational regional model”. *Advances in Meteorology,* 381630.

Lee YH, J Kim, J Hong. 2008. “The simulation of water vapor and carbon dioxide fluxes over a rice paddy field by modified Soil-Plant-Atmosphere model (mSPA)”. *Asia-Pacific Journal of Atmospheric Sciences*, 44 (1): 69-83.

Lhomme, JP. 1996. “A theoretical basis for the Priestley-Taylor coefficient”. *Boundary-Layer Meteorology*, 82:179-191.

Ministry of Agriculture, Food and Rural Affairs. 2013.

Moon SK, Y Ryu, D Lee, J Kim, JH Lim. 2007. “Quantifying the spatial heterogeneity of the land surface parameters at the two contrasting KoFlux sites by semivariogram”. *Korean Jurnal of Agricultural and Forest Meteorology*, 9(2): 140-148.

Park, S.B., Moon, S.K., Kim, J., Hong, J., Lee, Y., Lee, H.C., Choi, Y. 2006. “Haenam” KoFlux site. *AsiaFlux Newsletter*, 21: 19-21.

Priestley CHB and RJ Taylor. 1972. “On the assessment of surface heat flux and evaporation using large-scale parameters”. *Monthly Weather Review*, 100(2): 81-92.

Poley HW, HB Johnson, HS Mayeux, DA Brown, JWC White. 1996. “Leaf and plant water use efficiency of C4 species grown at glacial to elevated CO2 concentrations”. *International Journal of Plant Sciences,* 157 (2): 164-170.

Ramankutty N, AT Evan, C Monfreda, JA Foley. 2008. “Farming the planet: 1. Geographic distribution of global agricultural lands in the year 2000”. *Global biogeochemical cycles*, 22: 1003.

Reichstein Markus, JD thenhunen, O Roupsard, JM Ourcival, S Rambal, F Miglietta, A Peressottis, M Pecchiaris, G TIrone, and R Valentini. 2002. “Severe drought effects on ecosystem CO2 and H2O fluxes at three

Mediterranean evergreen sites: revision of current hypotheses?". *Global Change Biology,* 8: 999-1017.

Rosenberg NJ, BL Blad, SB Verma. 1983. "Microclimate the biological environment". John Wiley and Son, USA.

Ryu Y, S Kang, SK Moon, J Kim. 2008. "Evaluation of land surface radiation balance derived from moderate resolution imaging spectroradiometer (MODIS) over complex terrain and heterogeneous landscape on clear sky days". *Agricultural and Forest Meteorology*, 148: 1538-1552.

Schmid HP. 2002. "Footprint modeling for vegetation atmosphere exchange studies : a review and perspective". *Agricultural and Forest Meteorology*, 113: 159-183.

Sinclair TR, CB Tanner, JM Bennett. 1984. "Water-use efficiency in crop production". *BioScience*, 34: 36-40.

Song Y, Y Ryu, S Jeon. "Internannual variability of regional evapotranspiration under precipitation extremes: A case study of youngsan river basin in Korea". *Journal of Hydrology,* 519: 3531-3540.

Svirezhev YM. 2005. "Application of thermodynamic indices to agro-ecosystems". In SE Jorgensen. ed. "Ecological indicator for assessment of ecosystem health". Florida: CRC Press.

Svirezhev YM. 2008. "Entropy and Entropy Flows in the Biosphere". In SE Jorgensen. ed. "Encyclopedia of Ecology". The Netherlands: Elsevier BV.

Svirezhev YM and Svirejeva-Hopkins. 1998. "A sustainable biosphere: critical overview of basic concept of sustainability". *Ecological Modelling*, 106: 47-61.

Vickers Dean, CK Thomas, C Pettijohn, JG Martin, BE Law. 2012. "Five year of carbon fluxes and inherent water-use efficiency at two semi-arid pine forests with different disturbance histories". *Tellus B*, 64: 17159.

Wang E, CJ Smith, WJ Bond, K Verburg. "Estimation of vapour pressure deficit and crop water demand in APSIM and their implications for prediction of crop yield, water use and deep drainage". *Australian Journal of Agricultural Research*, 55: 1227 – 1240.

Williams CA, M Reichstein, N Buchmann, D Baldocchi, C Beer, C Schwalm, G Wohlfahrt, N Hasler, C Bernhof, T Foken, D Papale, S Schymanski, and K Schaefer. 2012. "Climate and vegetation controls on the surface water

balance: Synthesis of evapotranspiration measured across a global network of flux towers". *Water resources research*, 48: W06523.

Wolf Sebastian, W Eugster, C Ammann, M Hani, S Zielis, R Hiller, J Stieger, D Imer, L Merbold, N Buchmann. 2013. "Contrasting response of grassland versus forest carbon and water fluxes to spring drought in Switzerland". *Environmental Research Letter*, 8: 035007.

Xiao J, G Sun, J Chen, H Chen, S Chen, G Dong, S Gao, H Guo, J Guo, S Han, T Kato, Y Li, G Lin, W Lu, M Ma, S McNulty, C Shao, X Wang, X Xie, X Zhang, Z Zhang, B Zhao, G Zhou, J Zhou. 2013. "Carbon fluxes, evapotranspiration, and water use efficiency of terrestrial ecosystems in China". *Agricultural and Forest Meteorology,* 182-183, 76-90.

Yang D, F Sun, Z Liu, Z Cong, Z Lei. 2006. "Interpreting the complementary relationship in non-humid environments based on the Budyko and Penman hypotheses". *Geophysical Research Letters*, 33: L18406.

Yu G, X Song, Q Wang, Y Liu, D Guan, J Yan, X Sun, L Zhang, and X Wen. 2007. "Water use efficiency of forest ecosystems in eastern China and its relations to climatic variables". *New Phytologist*, 177: 927-937.

Appendixes

1. List of Eddy Covariance Measurement at HFK

System	open-path (CO2 flux, latent heat flux)
Wind speed	3D sonic anemometer (CSAT3, Campbell Sci., Inc., USA)
air temperature	3D sonic anemometer (CSAT3, Campbell Sci., Inc., USA)
water vapor	open-path (LI-7500, Li-Cor, USA)
CO_2	open-path (LI-7500, Li-Cor, USA)
Measurement height	20.8 m
sampling frequency	10Hz
averaging time	30 min
data logger	CR5000 (Campbell Sci., Inc., USA)
data storage	HD
original data	statistic

global solar radiation (incoming)	15m	CNR1 (Kipp&Zonen, Netherlands)
global solar radiation (outgoing)	15m	CNR1 (Kipp&Zonen, Netherlands)
long-wave radiation (incoming)	15m	CNR2 (Kipp&Zonen, Netherlands)
long-wave radiation (outgoing)	15m	CNR3 (Kipp&Zonen, Netherlands)
Net radiation	15m	CNR4 (Kipp&Zonen, Netherlands)
PPFD (incoming)	N/A	N/A
PPFD (outgoing)	N/A	N/A
direct/diffuse radiation	N/A	N/A
direct/diffuse PPFD	N/A	N/A
air temperature	20.8m	CSAT3 sonic anemometer (CSAT3, Campbell Sci., Inc., USA)
humidity	20.8m	LI-7500 (Li-Cor, USA)
soil temperature	~0.1m	2 TCAVs (Campbell Sci. , USA)
soil heat flux	~0.1m	2 HFP01SC (Campbell Sci. , USA)
soil water content	~0.1m	2 CS615 (Campbell Sci. , USA)
wind speed	20.8m	CSAT3 sonic anemometer (CSAT3, Campbell Sci., Inc., USA)
wind direction	20.8m	CSAT3 sonic anemometer (CSAT3, Campbell Sci., Inc., USA)

barometric pressure	19.5m	LI-7500 electronic box (Li-Cor, USA)
precipitation	surface	
CO2 concentration	20.8m	LI-7500 (Li-Cor, USA)
H2O concentration	20.8m	LI-7500 (Li-Cor, USA)

2. Comparison of Climate Condition with Climate Normal

Time	T_a (°C)			$R_{s\downarrow}$ (MJ m^{-2})			*VPD* (hPa)			*P* (mm)			Ws (m/s)		
	avg	std	cv	avg	std	cv	Avg	std	cv	avg	std	cv	Avg	std	cv
Winter	2.2	0.1	0.05	839	45	0.05	3.0	1.1	0.37	118	51	0.43	2.3	0	0.00
Spring	11.9	0.5	0.04	1541	100	0.06	5.7	1.9	0.33	350	89	0.25	2.9	0.1	0.03
Summer	24	0.7	0.03	1475	82	0.06	7.0	1.6	0.23	759	103	0.14	2.8	0.2	0.07
Fall	15.8	0.4	0.03	1170	28	0.02	6.3	1.9	0.30	243	102	0.42	2.1	0.1	0.05
Annual	**13.6**	**0.1**	**0.01**	**5025**	**154**	**0.03**	**5.4**	**1.6**	**0.30**	**1454**	**188**	**0.13**	**2.5**	**0.1**	**0.04**
The normal (1981-2010)	**13.4**									**1325**			**2.2**		

3. Annual Radiation Component at HFK

year	$R_{s\downarrow}$	$R_{s\uparrow}$	$R_{l\downarrow}$	$R_{l\uparrow}$	R_n	R_s_net	R_l_net	R_s net_anm	R_l net_anm	*EBR*
2003	4724	967	10882	12198	**2442**	3757	-1316	-240	115	**0.80**
2004	5215	1083	10794	12281	**2645**	4133	-1488	135	-57	**0.80**
2006	4952	983	10688	12276	**2380**	3969	-1588	-29	-158	**0.87**
2008	5078	1054	10855	12347	**2531**	4023	-1492	26	-62	**0.84**
2009	5162	1044	10799	12276	**2642**	4118	-1477	121	-46	**0.82**
2010	4872	966	10916	12220	**2602**	3906	-1303	-92	127	**0.87**
2011	5120	1129	10765	12161	**2595**	3991	-1396	-6	34	**0.90**
2012	5077	994	10812	12196	**2698**	4083	-1384	85	46	**0.83**

4. Soil Water Content Variation

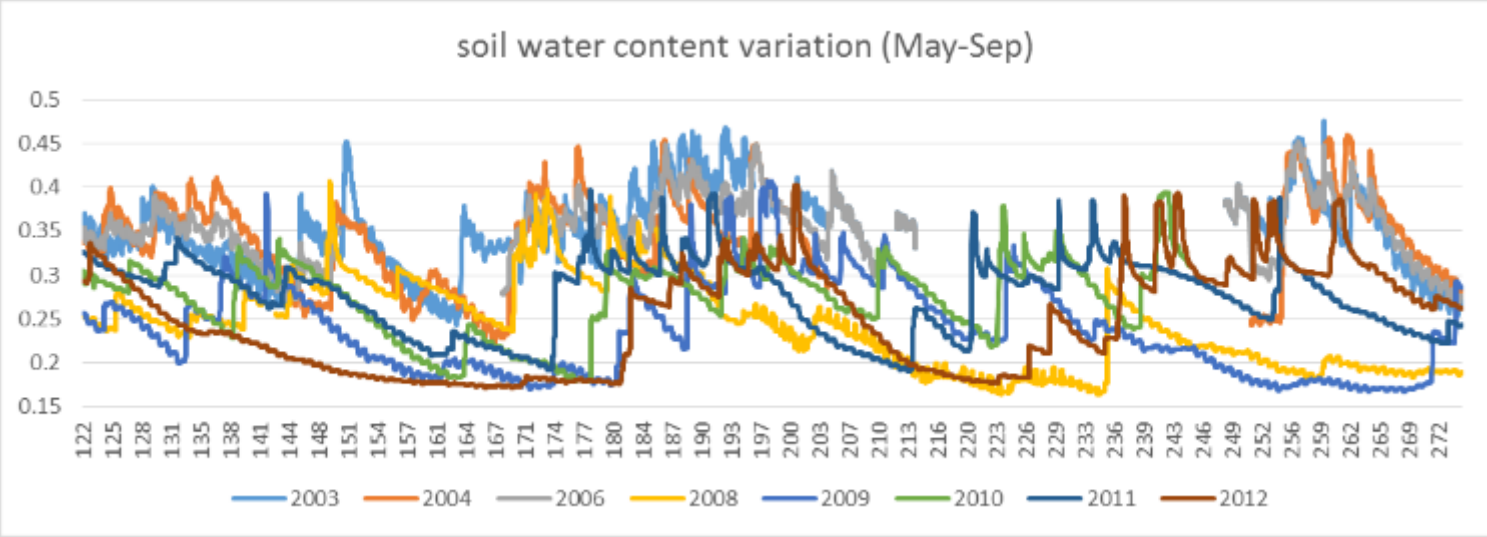

5. Land Cover Interpretation at HFK

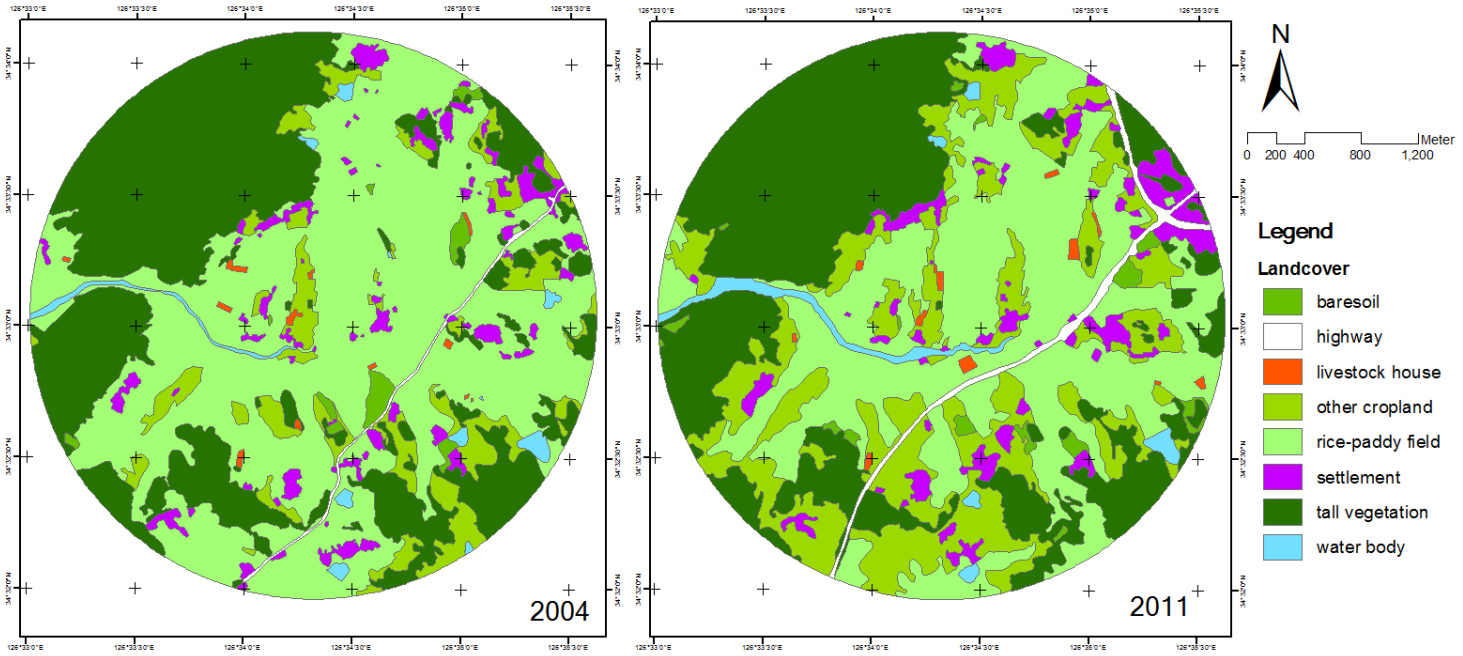

source: google map image (2011), Ikonos image (2004)

Abstract in Korean

초록

요하나
서울대학교 농업생명과학대학원
협동과정 농림기상학

인간의 개입 영향 하에 있는 현재의 농업생태계 관리 체계가 지속가능한 운영 및 관리를 추구하기 위한 적절한 방식인지를 판단하기 위해서는 생태계의 지속가능성 평가가 필요하다. 이 연구는 전형적인 농업생태계에서 관측된 장기 에디공분산 자료를 활용하여 특히 물 사용에 관한 생태계의 상태를 정량화하고자 하였다. 구체적인 연구 목표는 (1) 십 년 간의 기후, 물 사용, 에너지, 탄소수지를 문서화하고, (2) 이 농업생태계의 상태를 열역학적 관점에서 평가하는 것이다. 농업생태계의 물 사용의 현재 상태와 인간의 집중적인 관리 하에서의 그 역학을 어떻게 묘사할 수 있는지가 이 연구의 핵심 질문이다. 본 연구에서는 한국의 전형적인 농경지(해남 농경지, HFK)에서 십 년 간 관측된 에디공분산 플럭스 자료를 중심으로 사용하여 수행되었다.

평균 연간 강수량(P) 은 1454 ± 188mm였으며 이 중 여름에 내린 강수는 연간 강수량의 53 ± 5% 이었다. 연간 하향단파복사($R_{s\downarrow}$) 는 5025 ± 154 MJ m^{-2} 였으며 여름의 하향단파복사는 그 증감 양상이 강수와 반대의 양상을 보였다. 연평균 기온은 13.6 ± 0.1 ˚C 였고 점차 증가하는 양상을 보였다. 플럭스 발자국 기후도 분석에 따르면, 대부분의 관측된 플럭스 자료는 타워를 중심으로 약 200미터 이내에서 나타났다. 증발산에 대한 부디코(Budyko) 곡선은 연간 실제 증발산 (ET, 평균 639 ± 32 mm yr^{-1})이 가용에너지에 의해 제한됨을 보였다. 기준 증발산 (ET_o)의 평균은 728 ± 59 mm yr^{-1}였다. 벼의 성장기 동안의 평균 작물계수(K_c)는 0.88 ± 0.1 이었다. 초기 단계에 대한 통합된 작물계수는 0.87 ± 0.07 이었고, 발육 단계에서는 1.02 ± 0.08, 중기 단계에서는 1.02 ± 0.08, 그리고 후기 단계에 0.77 ± 0.10이었다. 연간 물사용효율(W_{ei})은 16.4 ± 3.6 gC kg H_2O^{-1} hPa로 나타났으며 큰 경년 변동으로 인하여 2004년에서 2008년 사이의 기간에서 더 높은 효율을 보였다. 탄소 수지에 대해서는, GPP, RE와 NEE의 평균이 각각 1235 ± 90, 1139 ± 54, −97 ± 119 gC m^{-2} yr^{-1}로 나타났다. 연간 총 순복사(R_n)의 평균은 2487 ± 238 MJ m^{-2} 였으며, 보웬비 (β)는 0.39 ± 0.05이었다. 에너지 수지 닫힘 비율 (EBR) 은 0.80에서 0.90사이의 값을 나타내었고 가장 높은 EBR은 2011년에, 가장 낮은 EBR은 2003 와 2004년에 나타났다. 내부 엔트로피 생산(σ)의 평균은 13.28 ± 0.47 MJ m^{-2} K^{-1} yr^{-1} 로 나타났다. 반면, 연 평균 엔트로피 수송(J)은 음의 값(−12.14 ± 0.38 MJ m^{-2} K^{-1} yr^{-1})으로서 이는 계 외부로 수송되는 엔트로피가 계 내부로 수송되는 엔트로피보다 큼을 나타낸다. 계 엔트로피의 시간당 변화율(dS/dt)은 증가하는 양상을 보였는데 2003년에 가장 낮았고(0.11 MJ

m^{-2} K^{-1} yr^{-1}) 2012년에 가장 높게 관측되었다(2.11 MJ m^{-2} K^{-1} yr^{-1}).

연구 결과에 따른 결론은 다음과 같이 요약할 수 있다.

(1) 증발산(*ET*)은 충분한 강수량과 지하수 등의 다른 물 공급원의 사용으로 인하여 물이 아니라 가용에너지에 의해 제한되었다.

(2) 작물계수(K_c)의 변동은 기준 증발산의 변동에 주로 관계되어 있었다.

(3) 물사용효율은 낮아서 생태계의 물 사용이 효율적이지 않음을 보였다.

(4) HFK 관측지에서의 물 사용 평가로부터 나타난 물의 비효율적인 사용은 이 농업생태계 내에서 발생한 엔트로피의 과다생산과 연관 지을 수 있다. 현재의 상황은 인간의 집중관리와 같은 인위적 교란의 증가로 시스템의 상태가 나빠지고 있음을 나타낸다.

주요어: 지속가능성, 열역학적 접근, 물 사용 ,농업생태계, 에디공분산 자료.
학 번 : 2013-22563.